# POLITECNICO DI TORINO

Department of Environment, Land and Infrastructure Engineering

Thesis to obtain the Master of Science degree in Petroleum Engineering

## Stochastic optimization of numerical Core flooding simulation



**Supervisor**

Prof. Vera Rocca

**Candidate**

Tailipu Mu

**Exchange University supervisors**

[ Instituto Superior Técnico — Lisbon, Portugal ]

Prof. Leonardo Azevedo

Prof. Gustavo Paneiro

Apr 2019

*This page is intentionally left blank*

## Abstract

Core flooding experiments are of great importance to study and evaluate the behavior of fluids in reservoir rock samples, providing useful insights to maximize reservoir productivity. These laboratory experiments often comprise an initial preparation step of routine core analysis to quantify the reservoir's porosity and permeability. The samples are then flooded with different fluids to mimic the natural physical phenomenon happening at the reservoir. The core sample is subjected to three different saturation states: first is saturated with brine, then oil then again with brine. This second step corresponds to core flooding analysis and aims assessing and evaluating the dynamic behavior of the core samples, mimicking the performance of the reservoir in depth, with the same condition of temperature and pressure but at a much smaller scale. The extrapolation of the small-scale behavior towards the field scale is not straightforward and is subject to geological and engineering uncertainties that may affect dramatically the description of the full-scale reservoir. This thesis also provides preliminary insights on how numerical fluid flow simulators are able to reproduce the lab experiments and how uncertainties can be assessed by stochastic optimization algorithms



**Key words**

Core flooding, permeability, saturation, reservoir simulation, numerical modeling, history matching, geological uncertainty, Particle Swarm Optimization.

*This page is intentionally left blank*

## Acknowledgements

First and foremost, I would like to thank Politecnico Di Torino and Instituto Superior Técnico (Lisbon) for offering me a platform and the opportunity in CERNA to apply my knowledge for preparing the last part of the study in the university (i.e. master thesis). Also, I am most thankful to Erasmus program for financial support for this study.

I am grateful to my supervisors Professor Leonardo Azevedo and Gustavo Paneiro, many thanks for their constant support, advice and guidance throughout this study. Special thank also goes to Professor Vera Rocca in Politecnico Di Torino, for her many helps, suggestions and corrections on this paper.

I also would like to thank PhD student Tosin for his help on simulation software during the studying process

And my thanks also go to the lab Specialist Mr. Fernandes for his help on the preparation of the core samples and other works in the lab.

During the reservoir simulation, some software and tools such as Petrel - Eclipse and RFD tNavigator are used for modelling, so my thanks also go to Schlumberger for their donation of the licenses on this software and tools. A software named Raven also has been used for history matching and optimization for reservoir parameters, therefore my special thanks also go to Epistemy for providing the software with its licenses.

Furthermore, I am greatly appreciating for the director, professors, personnel or staffs of CERENA for their assistance and support during my stay in Técnico Lisboa.

Finally, I would like to thank my family and all my friends for providing me the strength and moral support I always needed for getting through a very special phase of my life.

*This page is intentionally left blank*

# Table of Contents

# List of Figures

# List of Tables

# Nomenclatures

## Symbols, units and abbreviations

| | |
|---|---|
| $\mu$ | Fluid Viscosity, (Pa.s or cP) |
| $\upsilon$ | Fluid flow velocity, (m/s) |
| $\Delta P$ | Pressure drop, (Pa, bar or atm) |
| $\rho$ | Density, [$kg/m^3$ or $g/cm^3$] |
| $\Phi$ | Porosity |
| $\Phi_{min}$ | Minimum Porosity |
| $\Phi_{max}$ | Maximum Porosity |
| m | mass (kg or g) |
| A | Cross section area, ($m^2$ or $cm^2$) |
| D | Diameter (m or mm) |
| L | Length, (mm or m) |
| K | Permeability, (md) |
| $K_{abs}$ | Absolute permeability, (mD, Darcy or $m^2$) |
| $K_{min}$ | Minimum Permeability, (mD, Darcy or $m^2$) |
| $K_{max}$ | Maximum Permeability, ($m^2$ or Darcy $m^2$) |
| $K_{eff}$ | Effective permeability, (mD or Darcy or $m^2$) |
| $K_o$ | Oil permeability, ($m^2D$, Darcy or $m^2$) |
| $K_r$ | Relative permeability, (mD, Darcy or $m^2$) |
| P | Pressure, (Pa, bar or atm) |
| Q | Flow rate ($m^3/d$ or ml/h) |
| T | Temperature, (˚C) |
| V | Volume, (m3 or ml) |
| $V_b$ | Bulk volume, (m3 or ml) |
| $V_p$ | Pore volume of the core (m3 or ml) |
| ml | Milliliter |
| scc | Standard cubic centimeter |
| mm | Millimeter |
| cP | Centipoise (mPa.s) |
| mD | Millidarcy |
| $P_{in}$ | Inlet pressure (bar) |
| $P_{out}$ | Outlet pressure (bar) |

| | |
|---|---|
| $S_o$ | Oil saturation, fraction |
| $S_{or}$ | Residual oil saturation after water flooding, fraction |
| $S_w$ | Water saturation, fraction |
| $S_{wi}$ | Initial water saturation, fraction |
| ASP | Alkaline/surfactant/polymer |
| AC | Ant Colony |
| DE | Differential Evolution |
| EOR | Enhanced oil recovery |
| GA | Genetic Algorithm |
| IOR | Improved oil recovery |
| IFT | Interfacial tension |
| NA | Neighborhood Algorithm |
| OHIP | Original hydrocarbon in place |
| PSO | Particle Swarm Optimization |
| RCAL | Routine core analysis |
| RF | Recovery factor [%] |
| SCAL | Special core analysis |

*This page is intentionally left blank*

# Chapter 1 INTRODUCTION

## 1.1 Motivation

The petrophysical properties of the reservoir rock can be inferred by studying a core taken directly from the subsurface. Core analysis and core flooding can help to better understand the reservoir and evaluate the fluid behavior in the porous media. Often reservoir analogues from outcrops with similar rock properties as the reservoir are used to characterize the reservoir rock as core extraction is a costly process.

The direct measurements of the subsurface are scarce and costly, and the field can be produced only once. Numerical fluid flow simulators can be used to mimic the real reservoir fluid behavior and test different scenarios at very low cost. This is the reason why reservoir simulation becomes a widely used tool in reservoir management, especially for production forecasts. Some assumptions and pre-conditions are induced during the creation of the model and simulation process, obviously this leads to uncertainties, for instance geological uncertainty may introduced when scale the core size in lab up to reservoir size. Stochastic optimization method can help to assess and minimize this kind of uncertainty during the reservoir simulation.

This thesis aims at closing the gap between expensive and limited core flooding tests and numerical fluid flow simulation for better reservoir description and production optimization.

## 1.2 Objectives

The objective of this thesis is to better understand how conventional numerical fluid flow simulators are able to reproduce flow at the core sample. Core samples permeability and porosity are inferred by experimental core flooding over synthetic oil saturation, and stochastic history matching is carried out to reproduce the observed production at the core sample, then optimizing geologic parameters related to the geological description of the reservoir.

Under the scope of this work, Schlumberger software Eclipse 100® and RFD's tNavgator® were used as numerical fluid flow simulators, and RAVEN's Epistemy for stochastic optimization (i.e. stochastic history matching).

## 1.3 Structure of the thesis

This thesis is divided into the following chapters:

Chapter 1 is the introduction that includes the motivation and objectives related to the current work.

Chapter 2 reviews the main principles of core analysis, core flooding experiments, enhanced recovery techniques and reservoir simulation. This chapter also includes history matching with optimized reservoir parameters for future production forecast.

Chapter 3 describes core analysis and lab experiments in order to understand the laboratory data on core and its properties such as porosity and permeability; core flooding at lab scale was carried out as well to obtain the production data and analyze the fluid behavior in porous media in analogue samples.

Chapter 4 shows the numerical fluid flow simulation, where a simplified rock model was generated to be history matched with the production data obtained in the laboratory. History matching process was carried out by optimizing the reservoir parameters such as porosity and permeability. Particle swarm optimization was used as stochastic optimization technique, part of the history matching.

Chapter 5 reviews and summarizes the outcome from the reservoir simulation and history matching

This work was developed and executed in the Laboratory of Geosciences and Geotechnologies (GEOLAB) of CERENA (Center of Natural Resources and Environment) at Instituto Superior Técnico – Universidade de Lisboa, between November 2018 and March 2019. Mobility program of Politecnico Di Torino provide the financial support for this study.

*This page is intentionally left blank*

# Chapter 2 Literature Review

## 2.1 Core and Core Analysis

Core is a direct sample of the subsurface, and core analysis is a quantitatively measure of the core properties in the lab. Core can be used to simulate the reservoir condition in the lab. This can lead to be a better understanding of the hydrocarbon in place to provide some information for decision about the field development strategies.

The most important and basic information about the petrophysical properties of the reservoir normally are retrieved from the core. Rock properties such as porosity and permeability are determined by performing laboratory analyses on the cores from the reservoir to be evaluated. Routine Core Analysis (RCA) or Special Core Analysis (SCA) is the typical laboratory work to carry out to get those data (Tavakoli, 2018).

Core of the reservoir is collected during the drilling activity, but this operation is a costly process and sometimes analogue outcrop samples with the similar properties as the reservoir rock are used.

The core is normally a small cylindrical sample and called “Core plug” or just a plug. Plug dimensions are dependent of the core flooding apparatus. Figure 1 shows a typical core plug with 30 mm diameter and 100 mm in height, used in the work and made available by the Geo-Lab from CERENA (Instituto Superior Técnico).

Figure 1 Core sample with 30mm diameter and 100mm height

Porosity and permeability are key properties to model and describe the fluid flow in the reservoir and can be quantified by core analysis following standard laboratory procedures (Franklin, 1977).

### 2.1.1 Porosity

Porosity is a measure of the capability of storage (pore volume) of a given rock to hold fluids. It can be expressed by the ratio between the pore volumes and the total volume (bulk volume) of the specimen (Amyx, 1960). This important rock property can be obtained by the following generalized relationship:

$$\emptyset = \text{pore volume} / \text{bulk volume} \tag{2.1}$$

where $\emptyset$ = porosity

Some voids are interconnected and some are isolated impacting the fluid flow in the reservoir. One can consider two types of porosity, namely total porosity and effective porosity.

Total porosity is the ratio of the total pore space in the rock to the bulk volume. A rock may have considerable total porosity and yet have no conductivity to fluid for lack of pore interconnection (Cossé, 1993). The total porosity is generally expressed by the following relationships:

$$\emptyset t = \frac{\text{Total pore volume}}{\text{bulk volume}} \tag{2.2}$$

or

$$\emptyset t = \frac{\text{Bulk volume} - \text{Grain volume}}{\text{bulk volume}} \tag{2.3}$$

where $\emptyset t$ = total porosity

Effective porosity is the ratio of interconnected pore space to the bulk volume,

$$\emptyset \text{e} = \frac{\text{Interconnected pore volume}}{\text{bulk volume}} \tag{2.4}$$

where $\emptyset$e= effective porosity

Porosity in rock samples can be estimated in the laboratory by following ISRM suggested methods as below (Franklin, 1977):

a) The bulk volume of the specimen $V_{bulk}$ is calculated from an average of several caliper readings for each sample, by the formula below

$$V_{bulk} = L*(\pi D^2) / 4 \quad (2\text{-}5)$$

where D=diameter of the sample (m, or mm)

L=length of the sample (m, or mm)

b) Determination of void volume (i.e. pore volume)

The sample is saturated by fluid immersion in a vacuum with a pressure of 0.4 bar for 1 hour at least, and its saturated-surface-dry mass $M_{sat}$ can be measured. And then the sample is dried to a constant mass at a temperature of 105 °C, this is dry mass, or grain mass. Therefore

$$V_p = \frac{Msat - Ms}{\rho} \quad (2\text{-}6)$$

where $V_p$=pore volume($m^3$)

$M_{sat}$= saturated-surface-dry mass (kg)

$M_s$= Grain mass (kg)

ρ=Fluid that used for saturation ($kg/m^3$)

c) Porosity calculation

$$\Phi = \frac{Pore\ volume}{Bulk\ volume}$$

The porosity here refers to effective porosity since the determined pore volume here is interconnected void space.

The effective porosity is the one that is mostly used value by reservoir engineers for the calculations of plausible, probable and reserves. This is the key petrophysical property because it relates to the movable fluids through interconnected pore space.

Therefore, particular attention should be paid to the methods used to determine porosity. For instance, for effective porosity one can compute the weight difference between a fully saturated core sample (with a fluid of know density) and the dry core. This allows

computing the percentage of interconnected pore space. In a reservoir mode the original hydrocarbon in place (OHIP) is determined by the effective porosity (McPhee et al., 2015).

### 2.1.2 Permeability

Permeability is a very important parameter of the rock. It is the capacity and ability of the rock to allow the fluids to pass through. The permeability, k, manages the directional movement and rate of the fluids in the porous media (Amyx, 1960).

The definition of the permeability was introduced first by Henry Darcy in 1856, so called Darcy's law.

Darcy´s law, represented by the flow equation (2-5), becomes one of the standard mathematical tools for the reservoir engineer. In Darcy's equation, the fluid that flows through a core is considered as an incompressible fluid in a horizontal linear flow. Being the length of the core L, and its cross section of area A, the fluid flow equation can be expressed as

$$Q = -\frac{kA(p1-p2)}{\mu L} \tag{2-7}$$

where Q=flow rate, $m^3/s$

$\mu$= viscosity of the flowing fluid, Pa.s (or cP)

k= permeability, $m^2$ (or Darcy)

A=Cross section area, $m^2$

P1= Inlet pressure, Pa (or bar)

P2= Outlet pressure, Pa (or bar)

L=Length of the core, m

This equation is valid under the following conditions (Graue, 2006):

a) The core should be fully saturated with one-phase fluid;
b) There is no reaction between the core and the fluid;
c) The fluid which flows through the core should be addressed as steady-state laminar.

SI unit of the permeability is $m^2$, but the use of Darcy is very common. One given the scale of the fluid flow through a porous rock, millidarcy ($10^{-3}$ Darcy) is commonly used and 1mD = $10^{-15}$ $m^2$

Darcy equation 2-5 normally is exploit to the form of $k = \frac{Q\mu L}{A(p1-p2)}$ to calculate the rock permeability.

When a rock fully saturated with a single-phase fluid, the permeability is a rock property and not a property of the flowing fluid. This permeability is called absolute permeability (Lyons, 1996)

Permeability of the rock can be affected by the size of its grain and its structure, bigger size of the grain contributes higher permeability, for example fine grain sand stone has low permeability than course grain sandstone (Graue, 2006).

Standard laboratory analysis procedures should be followed in order to get a reliable data for the permeability of the core, (Ahmed, 2001).

There are some possibilities of having errors when determining the permeability. For example, the increases of the overburden stress will decrease the permeability of the rock in the case of having deep well. Incomplete core recovery also will affect the accuracy of the permeability.

## 2.2 Core flooding analysis

As previously mentioned, core analysis plays important role in understanding the subsurface reservoir. Costs may increase to a very high number for core extraction, transportation and other type of works until to get a desired shape of core. To utilize each core efficiently, some standardized methods are set across the industry, mainly categorized into 'Routine Core Analysis' (RCA) and 'Special Core Analysis' (SCA). (Tavakoli, 2018)

Routine core analysis is carried out in order to characterize the porosity, permeability and saturation. Whereas, Special Core Analysis centers around pore throat distribution, wettability, capillary pressure and other complex factors. But generally speaking, RCA cost less and performs faster compare to the SCA (McPhee, 2015)

Core flood analysis is the operation of injecting fluid(s) into the core and analyze the response of it. However, it is important to stress that the flow behavior obtained by core flooding in the lab represents the answer of the reservoir rock at a much smaller scale compared to a reservoir's size. Figure 2 is simplified core flooding model. The dimension

of the core and the viscosity of the flowing fluid are assumed to be constant during the test, but flow rate and injection pressure can be changed.

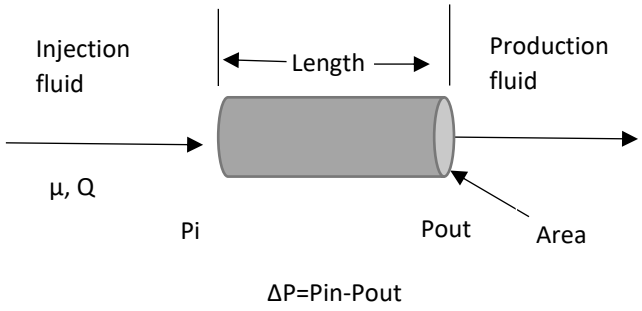


Figure 2 Simplified core flooding model

Core flooding experiments can be carried in different ways depending on the requirements of specific applications or the availability of the interpretation methods. Core flooding test can be done under the conditions of constant pressure difference across the core samples. This leads convenience for mathematical model to interpret the experimental data. Nevertheless, maintaining constant pressure difference and constant flow conditions is not easy in the actual test conditions and may not be fully completed, even though the high-quality equipment is used (http://www.oilfieldwiki.com).

Therefore, certain interpretation methods are preferred which can allow for variable flow conditions. Core flooding experiments can be carried out by using single or multiple core holders. Multiple core holders may be run in parallel or series depending on the specific reasons. For example, core plugs may be connected in series in order to simulate the effect of formation damage over long distance (http://www.oilfieldwiki.com).

### 2.2.1 Core flooding Procedure

Generally, for reservoir plugs, Routine Core Analysis considers the following steps (Avasare, 2016):

a) Clean the core sample (i.e. flushed by toluene first, then cleaned with ethanol).
b) Core drying process followed after cleaning. It can be done by many different ways, for example injecting with nitrogen ($N^2$), or leave it in the high temperature oven for

a time period (often 24 hours according to ISRM suggested method). Then the dry weight is measured.

c) The core can be saturated with desired fluid, for example with formation brine, then flooding with same formation brine until constant pressure drop is established. Permeability measurements is performed on the core, and this is absolute permeability.

d) Perform crude oil flooding until the saturation is achieved, and then set the temperature as reservoir to mimic the subsurface condition and followed by aging. The aging period can be various but at least two weeks (Avasare, 2016). This step is to ensure the core reaches the initial water saturation ($S_{wi}$) condition.

Figure 3 shows a core flooding test apparatus, designed and assembled for core flooding experiments (Rabiei, 2013).

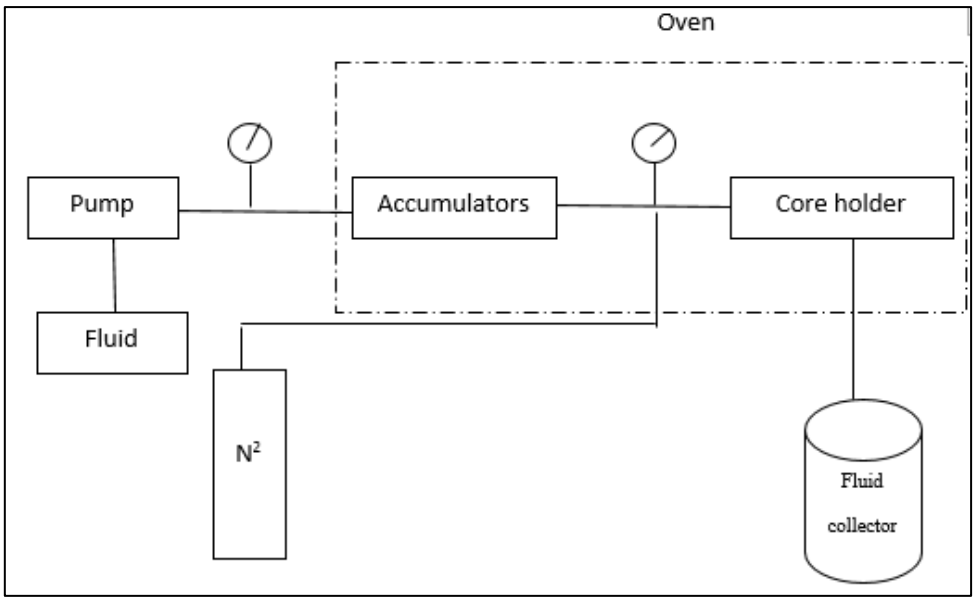


Figure 3 Simplified schematic of core flooding test (Adapted from Rabiei, 2013)

The test apparatus mainly includes a pump with injection rate from 0.01 up to 10 ml/min (Rabiei, 2013), a core holder and accumulators (for different fluid such as brine, crude oil, etc. by separately) were set in a temperature-controlled oven. The equipment in the core flooding apparatus can be various due to the different requirement and lab conditions.

## 2.3 Reservoir simulation

Reservoir simulation is a field developed in petroleum engineering where it can help to estimate the fluids dynamics by simulating porous media in computer modeling. Its goal is to predict the field performance under different producing strategies. This can be achieved since the field can be produced only once, but a model can be produced, or run, many times at very low expense over a short period of time. That is why reservoir simulation becomes a widely used tool in modern reservoir management, and it is the one of the basic tools applied by all reservoir engineers.

Building and maintaining a robust, reliable model of a field is normally expensive and time-consuming, models are typically only constructed where large investment decisions are made. Indeed, reservoir simulation has a bright future, and continuing investment in this technology will result long-term rewards for the industry (Gilman and Ozgen, 2013).

Applying and developing the new simulation technology provides a competitive advantage. Also, some simple reservoir simulators connected with many of today's basic reservoir-engineering software packages because of the low cost of hardware, for example well-testing and material-balance calculations.

A numerical fluid flow simulator (frequently designated as reservoir simulator) is a program that solves a group of equations where dynamic processes of the fluid flow are mathematically described, mimicking the real behavior of fluids in porous media in time and in three physical dimensions. The flow equations used to describe flow in porous media are based on mass, energy conservation equations and momentum, furthermore constitutive relations for the fluids and the porous media involved. By choosing the proper input data (e.g., fluid properties and reservoir rock) and the suitable solution of the mathematical equations, the performance of petroleum reservoirs can be simulated (or mimicked). In other words, it is possible to use a computer to establish a virtual reservoir that can be drilled, produced, and managed.

There are many factors affecting this virtual world. For example, the accuracy of the mathematical description of the recovery process, the reliability of the input data, the numerical methods used to solve the equations, and the validity of the simplifying assumptions applied by the program developer or users.

While the set of input and output data for a particular application is the “model”, the computer program that solves the linearized set of equations is normally referred to as a “simulator,” Therefore, reservoir modeling is the process of incorporating data evaluations and interpretations into a numerical simulator and using the outcome for reservoir engineering and reservoir management purposes.

Typical reservoir simulators enable to simulate multiphase flow in heterogeneous reservoirs with spatial variations of reservoir properties including porosity, permeability, pay zone thickness, fluid saturation, also faults and multiple wells. Modern reservoir simulators allow inclusion of multi-stage fractures. Reservoir simulators connected with wellbore flow simulators enable to use flow rate/wellhead pressure to specify operating conditions.

Reservoir simulators are not only used for optimizing the field production performance, but also use for well completion design in order to maximize the well productivity. For example, a design in Figure 4 displays two completion models of a multi-stage fractured horizontal well in a US field. Option (A) shows a case of one fracture produced from each cluster of perforations, and option (B) shows another case of three fractures/branches produced from each cluster of perforations (Guo et al., 2017). Figure 5 illustrates the outcome of production forecast provided by a reservoir simulation run for case (A) and case (B). The simulation curves in Figure 5 shows that short term (less than 13 years) production will increase on short multi fractures/branches from each perforation cluster, and long term (more than 13 years) production will decrease for long single-fractures from each cluster.

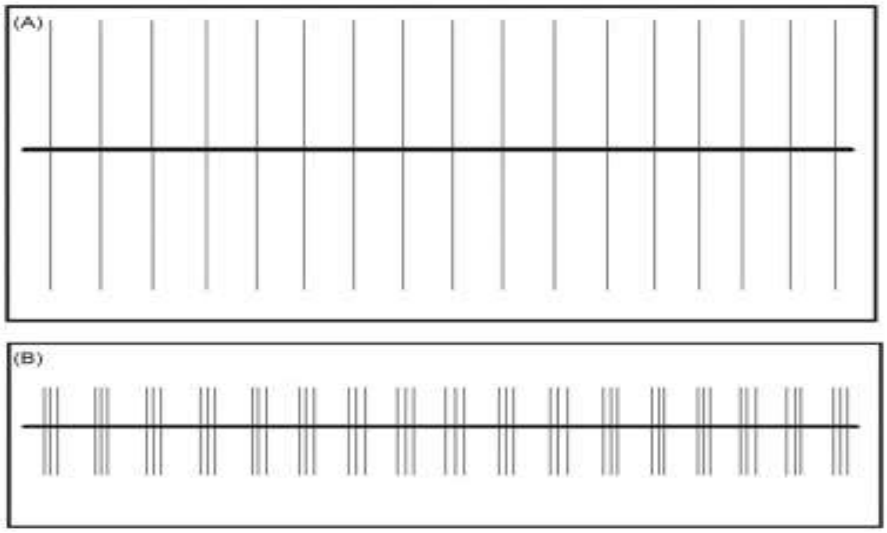


Figure 4 Two different completion models (Guo et al., 2017)

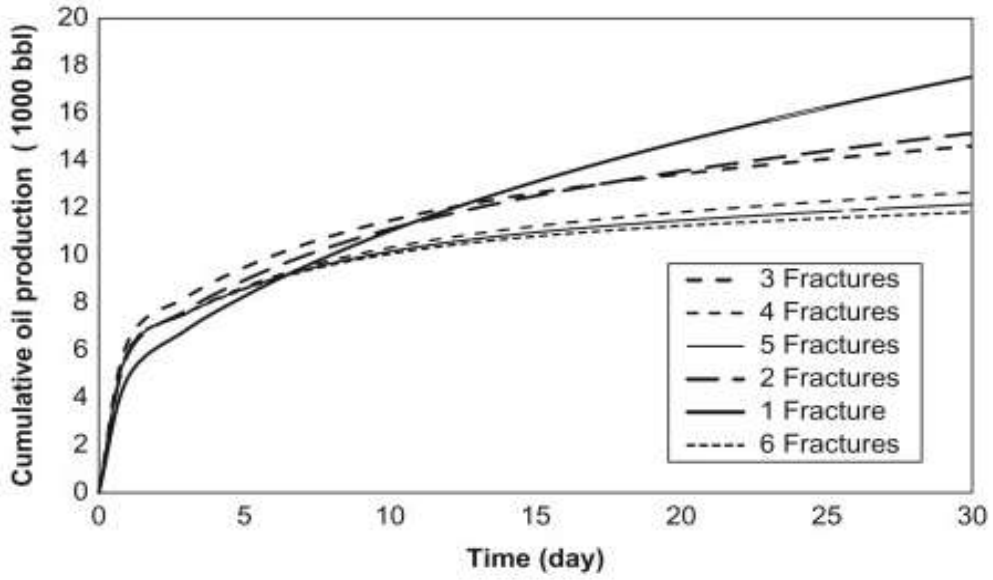


Figure 5 Production forecast by reservoir simulation for a multi-stage fractured horizontal well in a shale oil reservoir (Guo et al., 2017)

For every application, however, there is a custom-designed simulator. Every simulation study is different, starting from the reservoir description to the final analysis of results. Simulation is the art of combining mathematics, physics, reservoir engineering, and computer programming to develop a tool for predicting hydrocarbon reservoir performance under various operating strategies.

Numerical fluid flow simulations in reservoir engineering have several objectives, but mainly are the reservoir characterization, history matching and production forecast.

For reservoir characterization, some uncertainties must be handled after the establishment of the main characteristics of a hydrocarbon reservoir. These uncertainties maybe come from the data sources, or from limitations during the establishment of properties or geometry of the reservoir. A simulation model has the possibility to determine if production data or other types of dynamic data are compatible with the reservoir. As history matching is used in this thesis, the main concepts are introduced next.

## 2.4 History matching

History matching is the process that model parameters (such as relative permeability, fluid properties, geological description, etc.) are modified in such a way that simulated production data with these models match the real historical production data (production rates, pressures, tracers, temperatures, etc.). In fact, history matching is an exercise to calibrate the reservoir with the assumption that if a model is able to reproduce the history, it will help to predict the future under different development scenarios. This is the precondition of building simulation models and history matching them, and it is the only way to reduce the risk of failure which associated with decisions that are made under the data with uncertainty.

By doing history matching, the best way is to treat the history-matching exercise as an extension of the reservoir characterization process. When ran properly, history matching can minimize the uncertainties associated with the reservoir characterization. This will help the reservoir engineer to clearly understand the uncertainties and assumptions that have been incorporated in the reservoir characterization process. Figure 6 shows the general procedure for history matching (Ertekin et al, 2001).

The exercise of calibration includes the simulation model with some known historical data (input constraints), analysis of the response (output) of the simulator to see how it matches with some additional historical observations, and then deciding on how/what to modify the simulation model in order to have the better match. Each loop like this is called a run, as in a simulation run. What was changed in the model and what result was obtained should be recorded either manually or by run-tracking software.

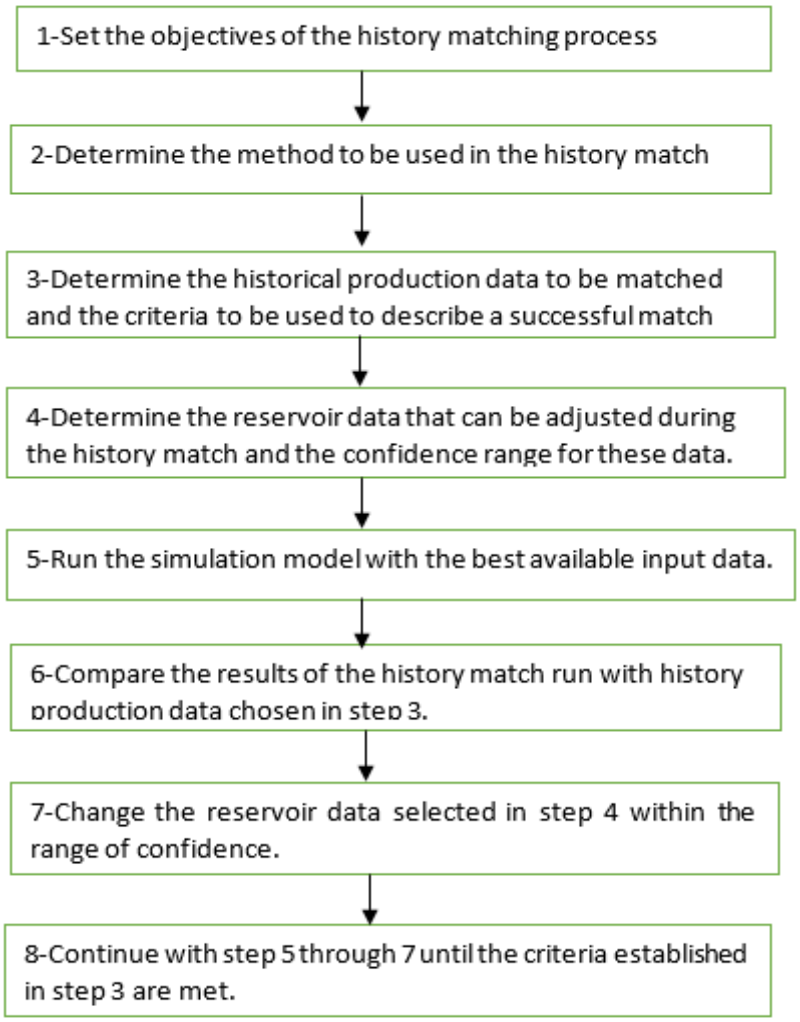


Figure 6 General procedure for history matching

Figure 7 illustrates the result of applying a typical history matching process after calibrating the model parameters (Done by simulator tNavigator). The dotted red curve above in the figure is history production data or observed data, and the lower solid red curve is simulated data. Further calibration and optimization can be done by altering the parameters in the model.

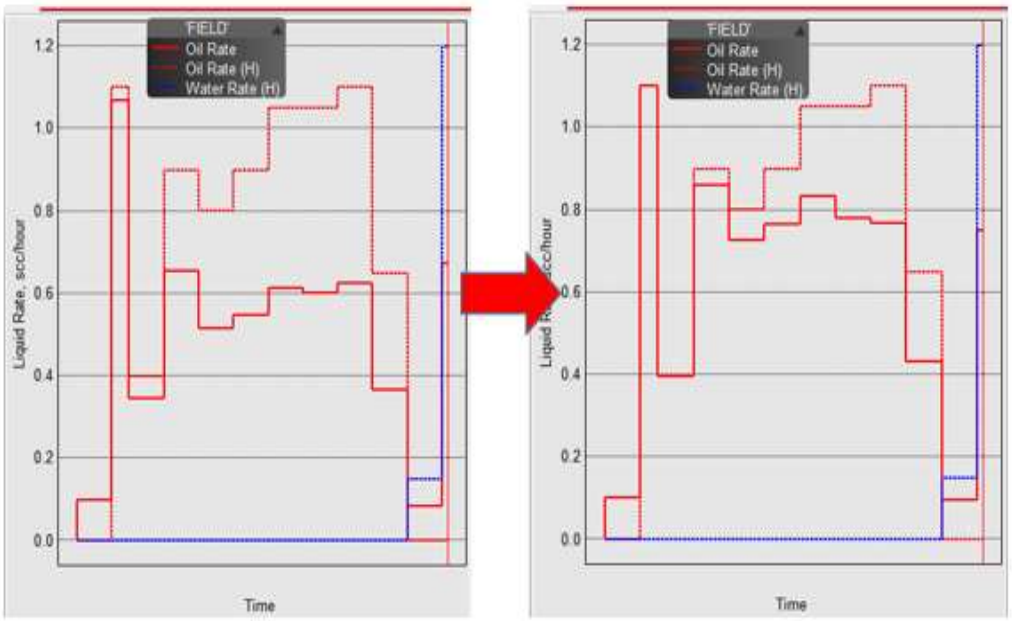


Figure 7 Typical History matching

There is no single standard method of determining the quality of the model calibration (i.e. the match between observed and simulated production data) = Each organization has their own way to evaluate the quality of the history match and even within an organization, each team may have different criteria. But the capability of forecasting the future performance is the final verification of the quality of the match. This capability is influenced by the method that is used during the calibration and reservoir characterization.

A simplified grid model shown in Figure 8 (Created by Petrel and displayed in tNavigator). The total dimension of the model in number of cells is 4*10*40=1600. This illustrates the reservoir grid used to mimic the core flood laboratory experiments.

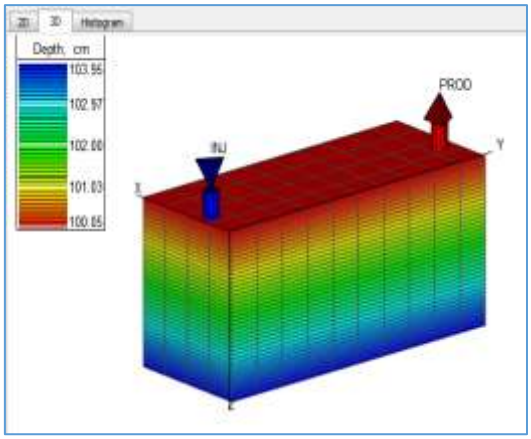


Figure 8 A simplified grid model for water flooding simulations

For instance, in a specific analysis, comparison needed for the forecast of an alkaline-surfactant-polymer (ASP) design for a heavy-oil reservoir with water flooding. Figure9 illustrate the data from core floods were used to establish the simulation inputs for relative permeability curves

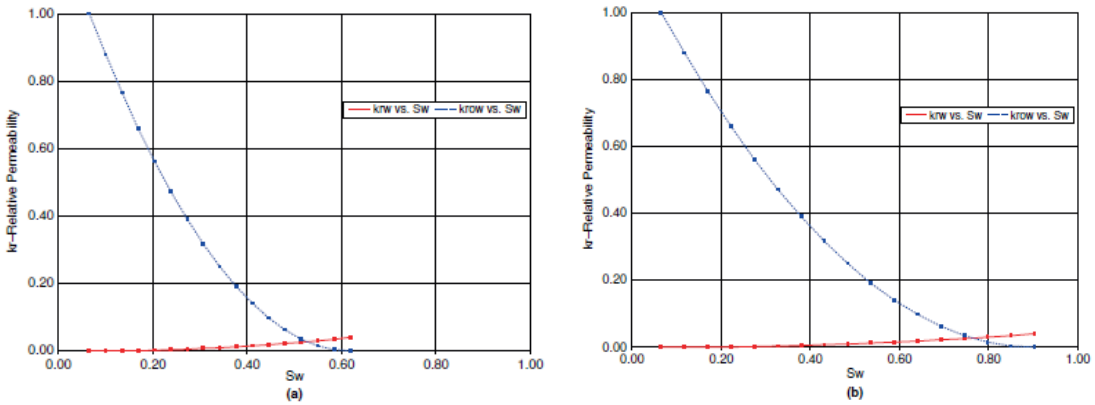


Figure 9 Low (a) and high (b) capillary numbers in relative permeability curves

For this case, a commercial simulator was used based on partitioning. This kind of software assumes smooth changes in relative permeability curves as the capillary number increases as the result of surface-active reagents such as surfactants. Figure10 (Created by tNavigator) is the water flooding cure that shows the cumulative oil production from the model in Figure 8.

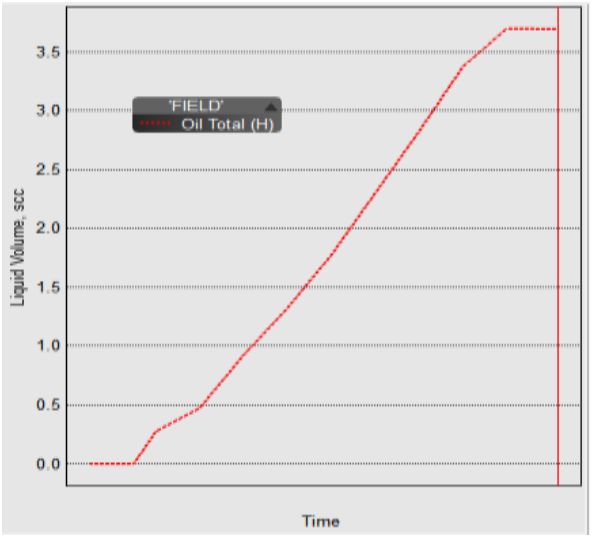


Figure 10 Cumulative oil production for water-flooding from the numerical reservoir model shown in Figure 8

2.4.2 Stochastic optimization

Stochastic techniques have been used in reservoir engineering since many years ago. This method including the algorithms of Ant Colony (AC)optimization, Differential Evolution (DE), Particle Swarm optimization (PSO) and Neighborhood Algorithm (NA).

The particle swarm optimization algorithm was firstly introduced by Kennedy and Eberhard (1995). It is a kind of stochastic optimization method inspired by the social behavior of fish schooling or bird flocking. It is proved that PSO can have better results in faster and cheaper way compare with other stochastic techniques like Genetic Algorithm (GA). It has been successfully applied in many fields, research and application areas, including petroleum engineering (Mohamed et al., 2010). Some years ago researcher worked on the comparison of Neighborhood Algorithm (NA) and PSO algorithm, and found that PSO has shown promising results in uncertainty quantification problems during the comparison of these two algorithms for finding acceptable multiple reservoir history matched models quickly (Muhamad et al., 2009).Furthermore, PSO is a conventional optimizer since it has a small number of parameters to adjust.

The PSO algorithm starts with a random position of a set of particles in the search space and moving them around in search for the best position according to a velocity vector. Each particle retains the memory of its previous best position in a personal vector while the best position among the swarm, called global best position, is stored in a global vector. When a new best position is achieved, it will influence the movement of the swarm and the velocity vector.

PSO exists in moving particles (vectors of size the number of parameters) in the parameter space to find the minimum of an objective function measuring a distance between the real data and simulated outputs. A particle *i* is moved randomly and iteratively in the parameter space and at same time keeping for iteration t + 1 the memory of its best experienced position $p_i^t$ between [0, t] and the memory of the best experienced position among all the individuals of the swarm gt (i.e. global position).

After assigning an initialization step to each particle a random location and a velocity in the parameter space, every iteration calculates the value of the objective function for each particle and updates velocities ($v_i^{t+1}$) and positions ($x_i^{t+1}$) Equations (2-6) and (2-7):

$$v_i^{t+1} = w.v_i^t + c_1.r_1(g^t - x_i^t) + c_2.r_2(p_i^t - x_i^t) \quad (2\text{-}6)$$

$$x_i^{t+1} = x_i^t + v^{t+1} \quad (2\text{-}7)$$

where *w* is the inertia weight, c1 and c2 are acceleration constants, and r1 and r2 are random number uniformly distributed in (0, 1). PSO is often considered as well-suited to nonlinear ill-posed inverse problems because its global search through the parameter space and the exchange of information between individuals lowers the risks of converging toward a local minimum.

# Chapter 3 Core flooding lab experiments

## 3.1 Preparation of core samples and fluids

### 3.1.1 Core sample

The core samples used for the lab experiments in this work were obtained from the rock shown in Figure 11(a). Rock samples were collected from a limestone quarry located in the center of Portugal, Figure 11(b). This is the largest limestone outcrop of Middle Jurassic found in the country (Carvalho et al., 2011). According to Rodrigues (1998), the geomorphological record that identifies Aire and Candeeiros mountains are the faults that affect it, resulting from tectonic movements.


(a) (b) (c)

Figure 11 Core and its source (a) Limestone outcrop (Almeida, 2018) (b) Geological position of the outcrop (c) Core samples collected from the outcrop

According to MOCAPOR, a Portugal-based company that works in the field of extraction and processing of natural ornamental stones, the limestone of the bounded area shows a bio-clastic component with micritic and esparitic cement, and dark grains dispersed throughout the rock. At the place indicated, there are light-colored carsic materials with small filaments of translucent calcite and reddish impregnations (Manuppella et al., 2006)

There is no any discovered reservoir associated with this type of limestone in Portugal so far, but it has similar property with Brazil pre-salt reservoir. This type of rock is used as analogue in many research and study works in the country. For example, some lab experiments such as triaxial test was carried out at Técnico Lisboa by Almeida (2018), Santos (2017) and Costa e Silva et al. (2014).

Seven samples were prepared for the core flooding test. However only five of them attended the formal lab experiments after preliminary test for first 2 core samples. Geometrical parameters were measured and listed in the Table 1.

Table 1 Geometrical parameters of the core samples

| Core Sample | Average Diameter (mm) | Average length (mm) | Section area ($mm^2$) |
|---|---|---|---|
| A1 | 37,156 | 101,772 | 1084,26 |
| A2 | 37,206 | 101,422 | 1087,18 |
| A3 | 37,286 | 101,65 | 1091,86 |
| A4 | 37,21 | 102,086 | 1087,42 |
| C1 | 37,134 | 100,85 | 1082,98 |
| C2 | 37,06 | 100,998 | 1078,67 |
| C3 | 37,05 | 100,908 | 1078,09 |

### 3.1.2 Samples preparation and Measurement

International Society for Rock Mechanic (ISRM) suggested methods protocol was followed for preparing the core samples in the lab.

Physical measurements were conducted very carefully on these samples. These include: the diameter, length and weight were measured five times per each and took the average number for the calculation in order to minimize the error. Figure 12 shows the tools for measuring the core sample.


Figure 12 Measurement of the core

Samples were put into the oven for drying with the temperature of 105° C for 17 hours, measured the weight of them, then put it back to the oven and measure the weight again after 4 hours and 7 hours to check for weight changes (Appendix A Table A-1). The weight measurements shown no changes after 17 hours in the oven for drying. For these reasons, samples were considered totally dried (Figure 13).

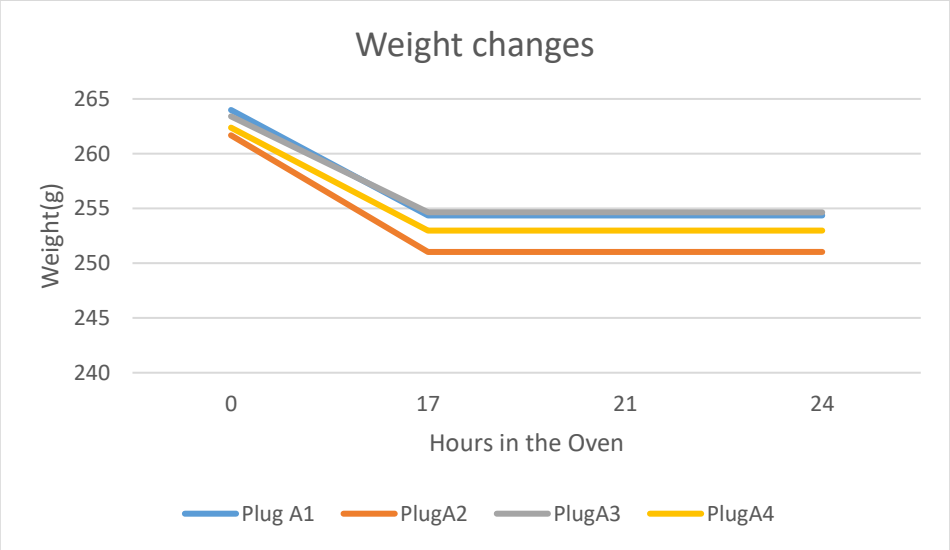


Figure 13 Weight differences during the drying

### 3.1.5 Porosity calculation

As mentioned earlier, ISRM should be followed for determining the porosity of the core. When the core sample is totally dried, all the water inside the pore is vanished, and then fully saturated by isooctane, we believe that all the connected pore spaces are filled by isooctane. Therefore, the amount of isooctane inside the pore can be computed by the weight difference, and the density of the isooctane is known, the volume of the isooctane can be obtained by very simple calculation, and this volume is equal to the effective pore volume of the sample.

Based on the geometrical data measured before, bulk volume of the core also can be computed very easily by a simple calculation. Since the porosity going to be used here is calculated based on the effective pore volume (i.e. interconnected pore space), therefore it is the effective porosity.

Same ISRM protocol was applied for porosity calculation process for all core samples, drying them in the oven for 24 hours and fully saturated with isooctane for 20 hours respectively, followed the same procedures and did the same treatment. The calculation results of porosity shown in the Table2.

Table 2 Porosity calculation results

| Core Sample | Bulk volume (m3) | Dry weight (g) | Wet Weight(g) | Weight difference(g) | Pore Volume(m3) | Effective Porosity |
|---|---|---|---|---|---|---|
| A1 | 1,10E-04 | 254,37 | 264,90 | 10,53 | 1,52E-05 | 0,138 |
| A2 | 1,10E-04 | 251,04 | 262,13 | 11,09 | 1,60E-05 | 0,145 |
| A3 | 1,11E-04 | 254,64 | 265,11 | 10,47 | 1,51E-05 | 0,136 |
| A4 | 1,11E-04 | 252,98 | 264,4 | 11,42 | 1,65E-05 | 0,148 |
| C1 | 1,09E-04 | 249,39 | 259,68 | 10,29 | 1,48E-05 | 0,136 |
| C2 | 1,09E-04 | 250,23 | 260,75 | 10,52 | 1,52E-05 | 0,139 |
| C3 | 1,09E-04 | 250,67 | 261,42 | 10,75 | 1,55E-05 | 0,143 |

Histogram shown in Figure17 is made based on the table above in order to have a better comparison.

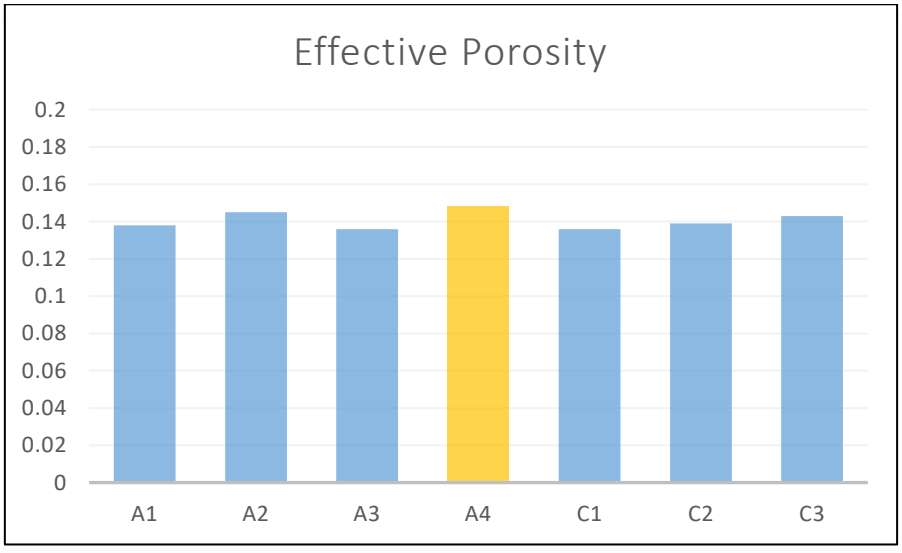


Figure 14 Effective Porosity of the core samples

Based on these data, important values such as mean value and standard deviation of the porosity were computed (Table3)

Table 3 some important values about the porosity among the populations

| | |
|---|---|
| Minimum Ø | 0,136 |
| Max Ø | 0,148 |
| Mean value of Ø | 0,141 |
| Standard deviation | 0,00443 |

Core sample A4 was treated differently, as it was fully saturated with isooctane for 23 days, the rest of the treatment are the same with the other core samples. This test aimed at evaluating possible differences if the core fully saturated with isooctane for 23 days instead of 20 hours.

### 3.1.3 Fluid preparation

Two type of fluids were prepared for the test, synthetic oil (i.e. Isooctane) and brine (i.e. NaCl mixed in distilled water). Synthetic oil isooctane is selected for the test since real reservoir oil is difficult to obtain to perform the investigation. However, synthetic oil like isooctane is easy to get and its property is known. On the other hand, isooctane has very low viscosity and easy to flow through the core sample with a relatively low injection pressure.

Isooctane is an organic compound with the formula $(CH_3)_3CCH_2CH(CH_3)_2$, shown on Figure 14. It is one of several isomers of octane ($C_8H_{18}$). This particular isomer is the standard 100 point on the octane rating scale (the zero point is n-heptane). It is an important component of gasoline.

The detail of the property of isooctane shown in the Figure 14 and table below.

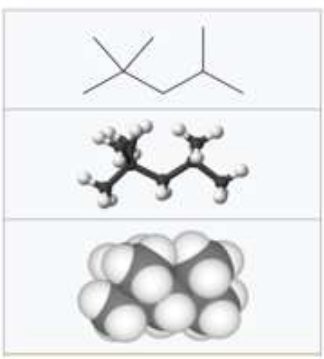

$C_8H_{18}= (CH_3)_3CCH_2CH(CH_3)_2$

| | |
|---|---|
| Molar mass | 114.2 g/mol |
| Density | 693kg/m$^3$ |
| Viscosity | 0.51 cP |
| Vapor pressure | 5.5kPa@21C$^0$ |

Figure 15 Main properties of Isooctane (Sources from Wikipedia and manufactures)

According to the International Programme on Chemical Safety (IPCS), Isooctane is flammable, and it can affect the people when breathed in. Therefore, it should be treated in very careful way during the test. And also keep it in safe and dark place after the test. It is also easy to evaporate, special care needs to be taken during the saturation and core flooding, for example evaporation should be avoid from the outlet during the production of isooctane when doing core flooding. Accurate reading of the production data is vital, and it becomes a bit challenge when an easy evaporate fluid flow like isooctane, especially when the flow rate is so small such as 2ml/hour. Therefore, a relatively smaller scaled cylinder is necessary (Figure 15) for measuring the amount of production, and the open end of this cylinder must be sealed to prevent the evaporation.

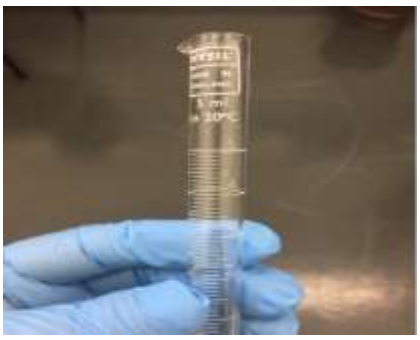

Figure 16 Fine scaled graduated cylinder

Brine is easy to prepare, this thesis used the brine with the concentration of having 35g NaCl in 1 liter of distilled water, it is about 0.6 moles NaCl, and the room temperature is about 20$^{o}$C, therefore the viscosity of the brine is estimated as 1.05 cP approximately according to the viscosity table (Kestin et al., 1981). It is higher than water, therefore it requires higher injection pressure for the core flooding operation compare to inject the isooctane.

### 3.1.4 Core saturation

A short discussion was held after the preparation of the core samples in the lab. ISRM suggested methods was introduced for core saturation process. The process was carried out in the vacuum equipment shown in Figure 16 by the following procedure:

a) Core plug is immerged in the isooctane by 2/3 of its length for one hour inside the vacuum device shown on figure under the pressure of 0.4 bar. This pressure helps the fluid moving into the pore space of the core

b) Fully immerge the core with isooctane for another one hour with the same condition, with the pressure of 0.4bar by vacuum pump.
c) Stop the pump and isolate the vacuum bottle from outside and leave the core fully immerge with isooctane for 18 hours.
d) Measure the weight immediately since the isooctane evaporate very fast

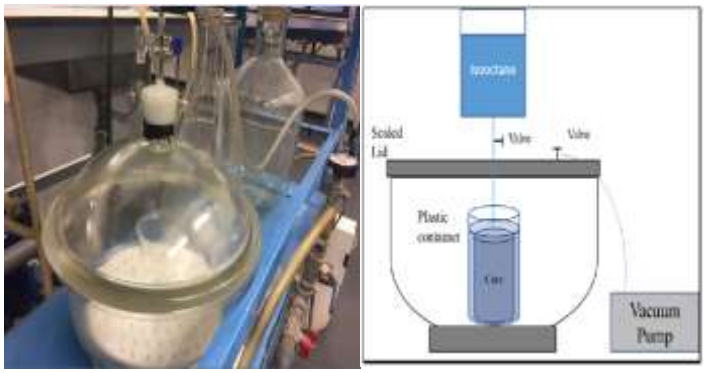


Figure 17 Vacuum equipment

### 3.2 Core flooding lab experiments

Core flooding lab experiments were divided in two parts. Firstly, isooctane saturated core was flooded with same isooctane in order to obtain the absolute permeability of the core sample by following Darcy's law. Secondly, same core was flooded with brine in order to mimic the reservoir fluid flow phenomena. Some important parameters and data were recorded in order to analyze the outcome, for example production data, injection pressure, confinement pressure and flow rate. Additionally, atmospheric pressure is considered as outlet pressure during the core flooding.

At the end, oil recover can be figured out by this process. Figure17 below is the simple illustrate of the core flooding.

#### 3.2.1 Equipment set up

Due to the lab equipment condition and limitation, the test was conducted in simple but effective way, the essential equipment such as injection pump, core holder, pressure

gauges and hydraulic hand pump are in line. A simplified experiment set up shown on Figure 18.

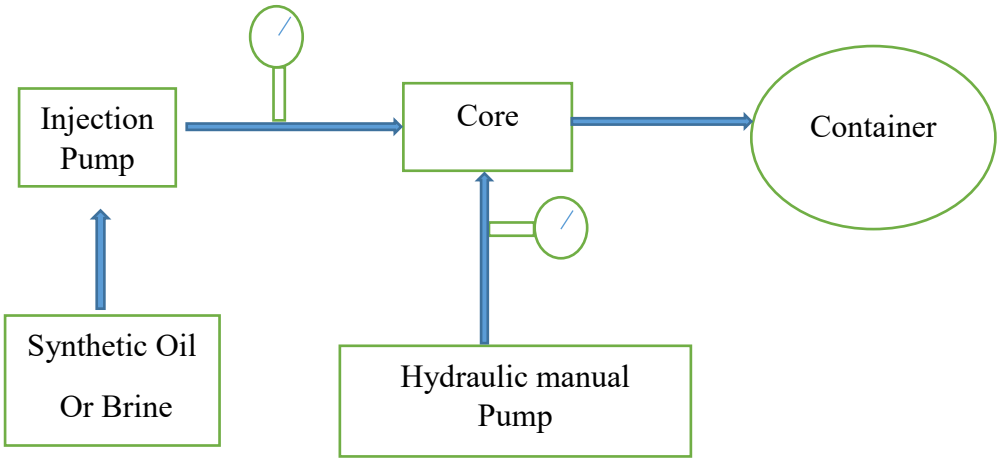


Figure 18 Core flooding set up

Main core flooding equipment shown on Figure 19 and Figure 20. The fluid injection pump (Figure 19a) has the pressure limitation up to 50 bars. The maximum injection pressure was set to 40 bar due to the consideration of safety. One extra pressure gauge was set in line between the pump and core holder as a reference check during the test, just in case the pressure indicator on the pump may get problem, or vice versa.

A hydraulic hand pump (Figure 19b) was introduced for providing the confinement pressure to the core holder in order to mimic the reservoir pressure during the test. Maximum pressure can be reach to 700 bar.


(a) (b)

Figure 19 Core flooding equipment (a) Fluid injection syringe pump (b) Hydraulic hand pump

Typical Hassler core holder (Figure20a) was used for the test. Figure20 (b) and (c) shows the inside of the core holder and the way of how it works

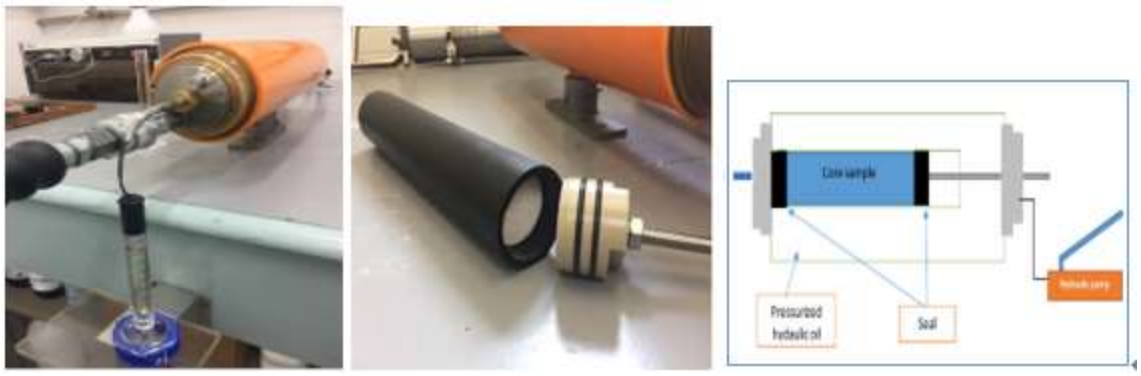


(a) (b) (c)

Figure 20 Hassler core holder

3.2.2 Core flooding with isooctane

Preliminary tests were carried out in order to get the proper parameters for the experiment, for example which confinement pressure and flow rate is better for the test. Initial working parameters planned as following:

Confinement pressure: 200 bar

Isooctane injection rate: 15 ml/hour, 20 ml/hour, and 25ml/hour

Brine injection rate: 9ml/hour, 3ml/hour and 2ml/hour

Injection rate was planned in such small number because of the limitation of the pump, maximum 40 bar is allowed during the test.

As mentioned before, those core samples came from same rock, therefore same condition and same ISRM protocol were applied for all of these samples, for example all of them were saturated with isooctane for 24 hours after totally dried in the oven.

First test started with core sample A1. Since the maximum allowable pressure of the pump to inject the fluid is about 40 bar due to its limitation, the flow rate of the

injecting fluid was decided carefully. Isooctane flooding was carried out first with the injection rate of 15ml/hour for 60 minutes under the confinement pressure of 200 bar, and then increased to 20ml/hour and 25ml/hour, the confinement pressure keep constant. The outcome shown in Table 4. The maximum injection pressure is about 19 bar when the flow rate was set to 25ml/hour, it is far less than maximum allowable pressure of the pump.

Table 4 Data from core flooding with isooctane for plug A1

| Core flooding with isooctane for Plug A1 | | | |
|---|---|---|---|
| Duration (minute) | Confine pressure (bar) | Flow rate (ml/h) | Inlet Pressure (bar) |
| 60 | 200 | 15 | 11.5 |
| 60 | 200 | 20 | 15 |
| 60 | 200 | 25 | 19 |

After that, core flooding with brine to same sample A1 was carried out under the same constant confinement pressure.

Relatively low injection rate was planned since the viscosity of the brine is much higher than isooctane and it will be more difficult to flow through the core sample. Injection pressure was almost reached the maximum allowable pressure of the pump and still keep increasing when the brine flooding was carrying out with the injection rate of 9 ml/hour and 3ml/hour (Table 5). This result shows the brine flooding is not doable with those parameters.

Table 5 Data from core flooding with brine for plug A1

| Core flooding with brine for Plug A1 | | | |
|---|---|---|---|
| Duration (minute) | Confine pressure (bar) | Flow rate (ml/h) | Inlet Pressure (bar) |
| 20 | 200 | 9 | >39 |
| 110 | 200 | 3 | >39 |
| 70 | 200 | 2 | 30 |

In order to find a better group of parameters for the core flooding experiments especially for flooding with brine, second test was conducted for core plug A2, adjusted parameters set for the second test as follow:

Confinement pressure: 100 bar

Isooctane injection rate: 15 ml/hour, 20 ml/hour and 25ml/hour

Brine injection rate: 3ml/hour and 2ml/hour

The results of the test are shown in Table 6 and Table 7.

Table 6 Data from core flooding with isooctane for plug A2

| Core flooding with isooctane for Plug A2 | | | |
|---|---|---|---|
| Duration (minute) | Confine pressure (bar) | Flow rate (ml/h) | Inlet Pressure (bar) |
| 60 | 100 | 15 | 10.5 |
| 60 | 100 | 20 | 15 |
| 60 | 100 | 25 | 18 |

According to the outcome above, isooctane flooding is fine to perform the test with those parameters.

Table 7 Data from core flooding with brine for plug A2

| Core flooding with brine for Plug A2 | | | |
|---|---|---|---|
| Duration (minute) | Confine pressure (bar) | Flow rate (ml/h) | Inlet Pressure (bar) |
| 340 | 100 | 3 | >39 |

But again, for the core flooding test with brine, the injection pressure is over the maximum allowable pressure to perform according to the result above in the Table 7.

After two tests above, proper flow rate and confinement pressure was set based on the discussion, shown in Table 8.

Table 8 Final parameters set for the lab experiments

| Confinement pressure for the core flooding: 100 bar | | | |
|---|---|---|---|
| Flow rate for isooctane flooding | | | Flow rate for brine flooding |
| Q1 (ml/h) | Q2(ml/h) | Q3(ml/h) | Q(ml/h) |
| 15ml/h | 20ml/h | 25ml/h | 2ml/h |

Core plug A3 was tested with the new work parameters above, the rest of core samples will be followed the same procedure and same parameters, and at the end the result will be compared.

Firstly, isooctane flooding test was carried out, and the permeability for each flow rate was computed based on the application of Darcy's equation

Since isooctane flooding was conducted in three different flow rates, thus there were 3 calculation results obtained respectively.

Figure 21 is the display of histogram for the result of absolute permeability based on different flow rate

Detail of the isooctane flooding and the results are shown in Appendix B Figure B-1.

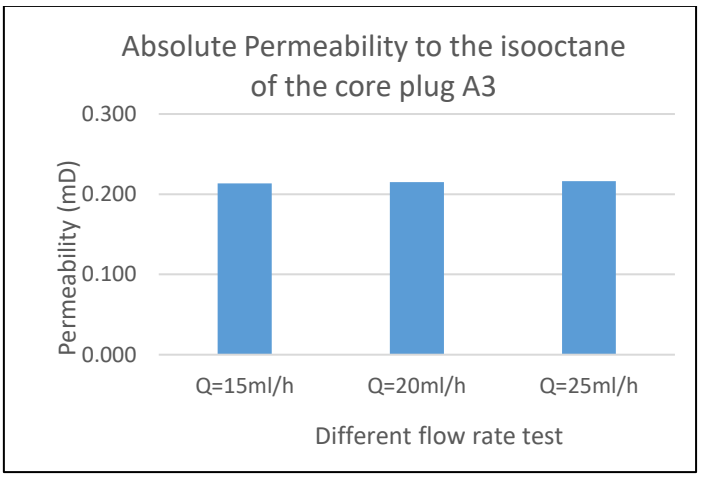


Figure 21 Permeability to the isooctane for the core plug A3 in different flow rate

Same isooctane core flooding tests were carried out for other four core samples. Computed result of absolute permeability for each core sample shows in Figure (22), and this is average absolute permeability of each core because the core was flooded by three different flow rate and three different results came out of the calculation (Figure 21). Detailed individual results of absolute permeability for each step rate test shown in the graph in Appendix B respectively.

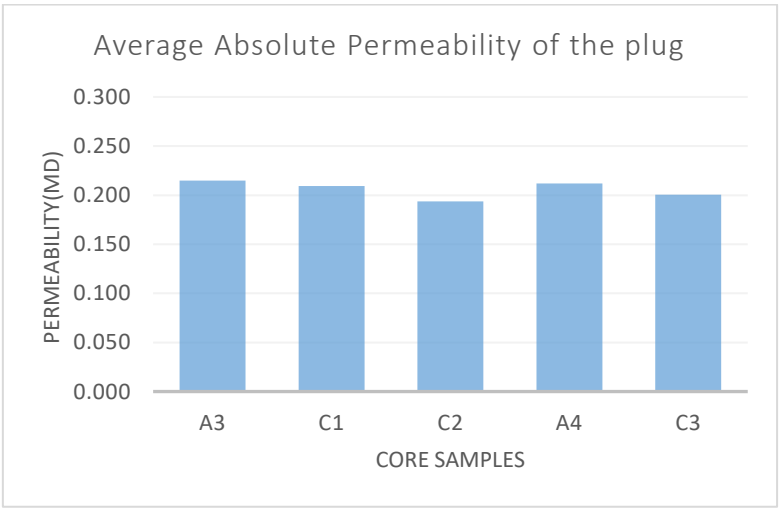


Figure 22 Average absolute permeability of each core sample

### 3.2.2 Core flooding with brine

Core flooding with brine was performed after the isooctane flooding. As mentioned earlier, flooding flow rate has to be decreased a lot compare to the isooctane flooding flow rate, because brine has much higher viscosity (about 1.05 cP) than isooctane (about 0.51 cP) , and it requires higher injection pressure to be able to proceed the flooding, and the injection pressure is restricted by the maximum allowable pumping pressure (i.e. 40bar). Therefore, working parameters for core flooding with brine was determined based on condition above by the following:

Flow rate Q=2ml/h confinement pressure $P_{conf}$=100 bar.

Since the flow rate is very small, it took the entire day in the lab to obtain the constant injection pressure. For example, the test for plug A3, it took about 8 hours from the pump started. The graph of injection pressure and production profile shows in Figure 23. The entire detailed production data of core flooding with brine for plug A3 is shown in Appendix C Table C-1

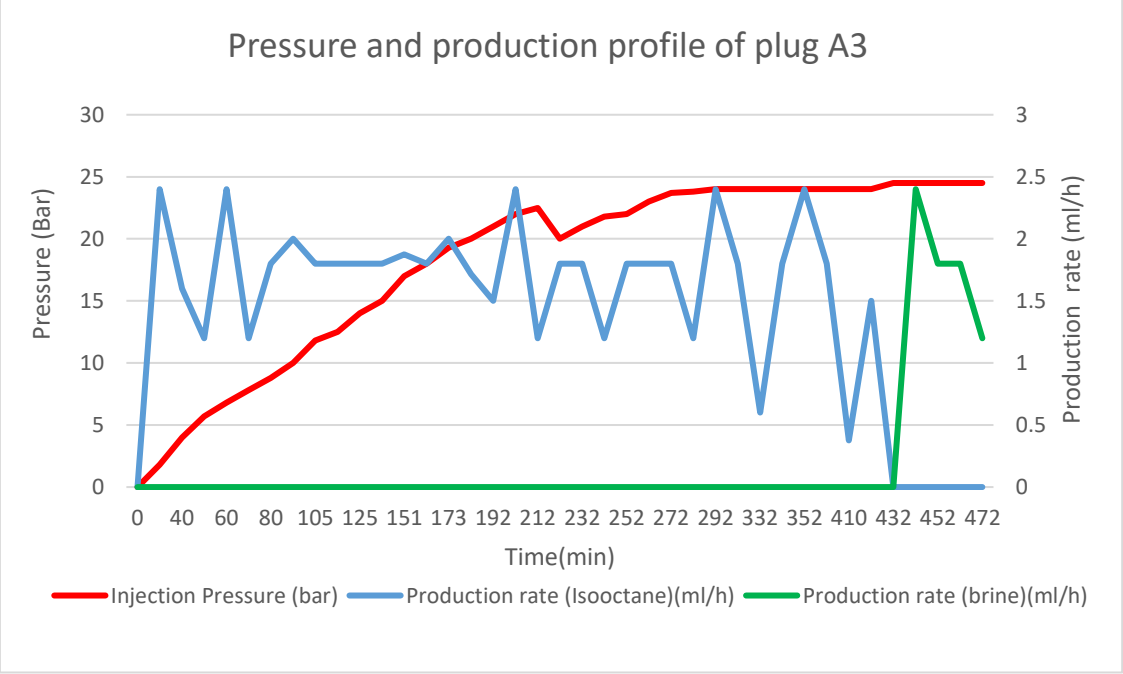


Figure 23 Pressure and Production profile of Plug A3

During the core flooding test, the production rate is not stable due to the natural heterogeneity of the core sample. From Figure 23 it is possible to interpret a pressure decline at a given moment followed by an increase. This phenomenon tells us maybe there are some mini fractures developed and connected inside the core during the core flooding experiment.

Core flooding with isooctane operation were carried out for other four specimens, Plug C1, Plug C2, Plug C3 and Plug A4, by following the same procedure and same working parameters which set before and applied for core plug A3 earlier. The results of pressure and production profile for each sample displays in the Figure24, 25, 26 and 27 respectively. For further detail information please refer the tables listed in Appendix C Table-C2, C3, C4, and C5 respectively.

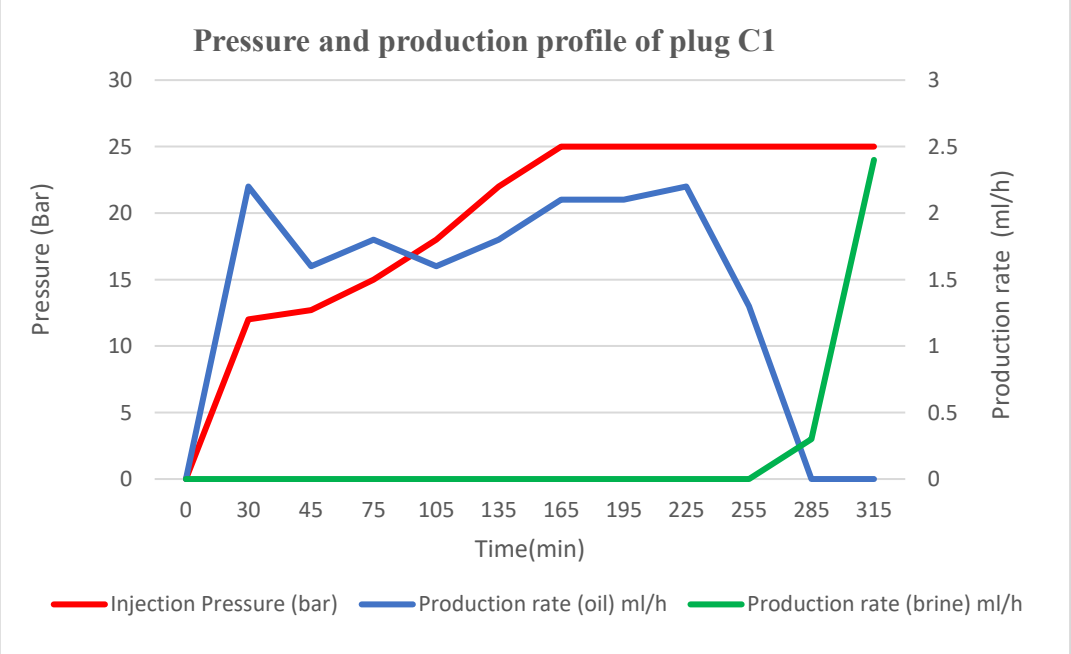


Figure 24 Pressure and Production profile of Plug C1

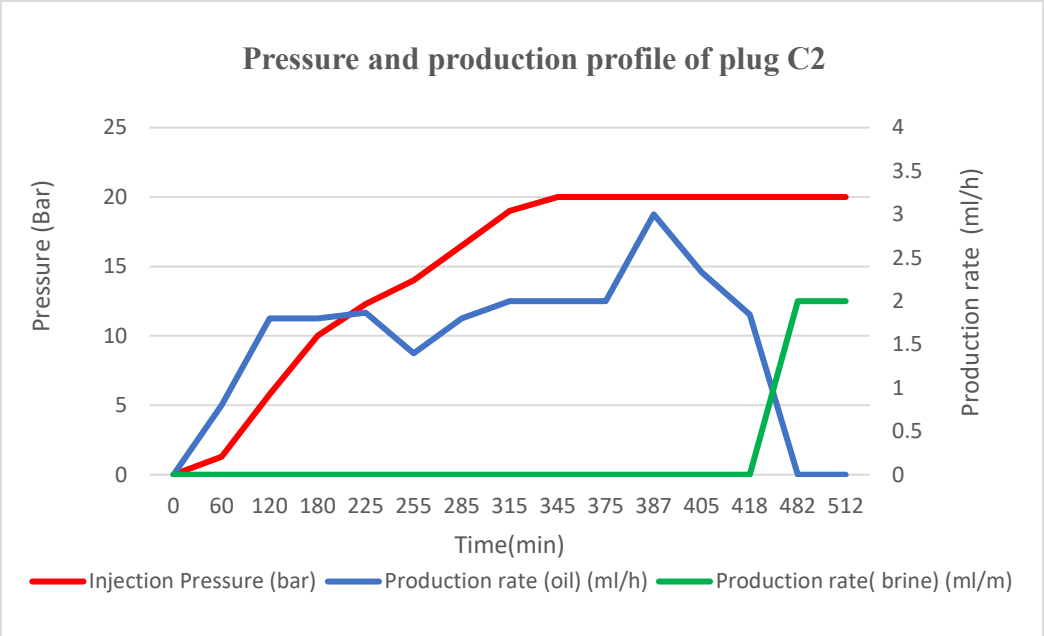


Figure 25 Pressure and Production profile of Plug C2

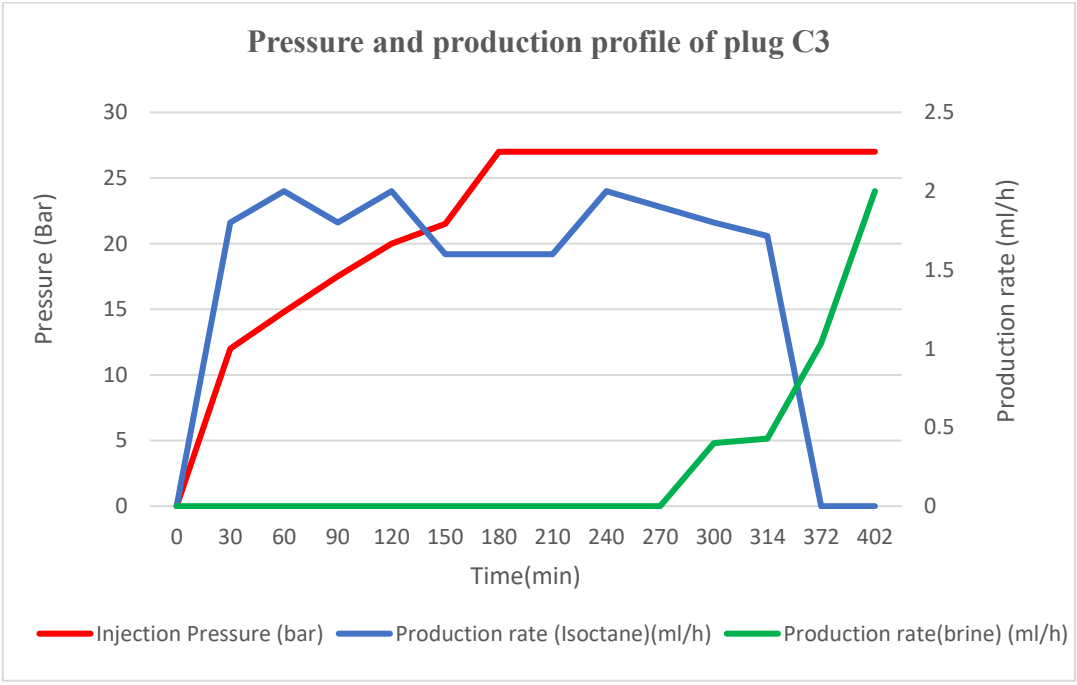


Figure 26 Pressure and Production profile of Plug C3

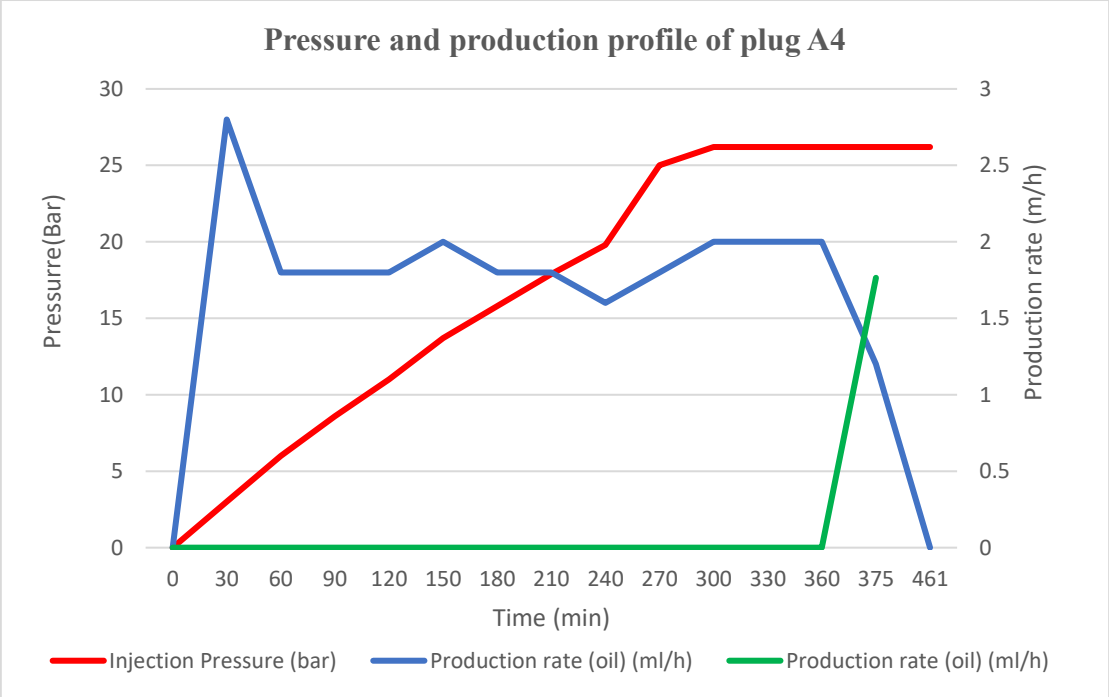


Figure 27 Pressure and Production profile of Plug A4

Some interesting phenomenon were observed during the brine flooding. There is always empty space or gap between the end of isooctane and the first brine produced from the outlet, sometimes it takes more than half an hour for nothing produced even though the injection rate and the pressure still keep constant from the other side of the core sample. The main reason for this is the properties differences of two types of fluid, for example they are not miscible because isooctane is organic phase non polar liquid, and brine is water phase polar liquid, as simple as we all know that oil and water do not mix (Silverstein,1998). On the other hand, isooctane has much lower viscosity than the brine, it is thin oil, so isooctane flows much easier and faster than brine in the core or pipe, and thanks to the interfacial tension as well the size of droplet of brine from the outlet can be seen is bigger than isooctane (Majod et al., 2015). Figure28 shows the brine comes out from the core and it occupied almost the whole pipe space when flowing.


Figure 28 Brine in the pip

One more thing observed, there is no isooctane produced anymore after the first brine comes from the outlet. This is due to the non-miscible nature of the two type of fluids. The heavy fluid brine pushed out the most of the movable light fluid isooctane from the core.

### 3.2.3 Relative permeability to the brine

As mentioned earlier, absolute permeability was estimated by single phase fluid flow though the rock sample, i.e. the core was fully saturated with isooctane and flooded by isooctane. And for flooding with brine we have two different fluids isooctane and brine in the rock sample, therefore the permeability obtained here by the application of Darcy´s law is the relative permeability to brine.

Relative permeability to the brine can be computed based on the following known parameters, again take the core sample A3 as an example:

Viscosity of the brine is 1.05cP which mentioned earlier;

Flow rate is 2ml/hour;

Length of the core is 101.65mm;

Diameter of the core is 37.29mm;

Stabilized injection pressure is 24.5 bar

Outlet pressure is atmospheric pressure 1 atm.

Therefore, the relative permeability to brine is computed by the Darcy equation below

$K=q*\mu*L / A*\Delta P$

$K_{rel}= (2*10^{-6} *1.05*10^{-15}*0.10165)/ (3.1415*0.01864^2*3600*(24.5*100000-101325))$ =0.0231 mD

If compare this relative permeability to brine with the absolute permeability (about 0.21mD) which obtained by isooctane flooding shown in Figure 21, it is about nine times less than absolute permeability.

### 3.2.4 Oil recovery factor

This experimental setup mimics an EOR technique at the lab scale, synthetic oil isooctane was flooded out from the core by brine, based on the production data collected during the test, the oil recovery i.e. recovery factor was computed.

Recovery factor = Cumulative oil production/Original oil in place

In our case, the core was fully saturated with isooctane, the amount of isooctane inside the core is known (i.e. equal to its pore volume), and the total amount of the produced isooctane also can be obtained after the core flooding test. The recovery factor here in this test is

RF=pore volume / total isooctane produced

Pore volume=15.1ml, Produced isooctane=10.8

Therefore, RF=10.8ml/15.1ml=0.715

The information and outcome from the core flooding test with brine is summarized in the Table9.

Table 9 Recovery factor for plug A3

| **Core flooding with brine for Plug A3** | | | | | | |
|---|---|---|---|---|---|---|
| Duration (minute) | Confine pressure (bar) | Flow rate (ml/h) | Stabled Inlet Pressure (bar) | Pore volume (ml) | Total produced isooctane (ml) | Recovery factor |
| 402 | 100 | 2 | 24.5 | 15.1 | 10.8 | 0.715 |

Oil recovery was estimated for each sample at the end of the core flooding process. The ratio of produced oil to pore volume of the core is defined as recover factor. The results shown in Figure 29. Detailed table is in the list of Appendix A Table A-4

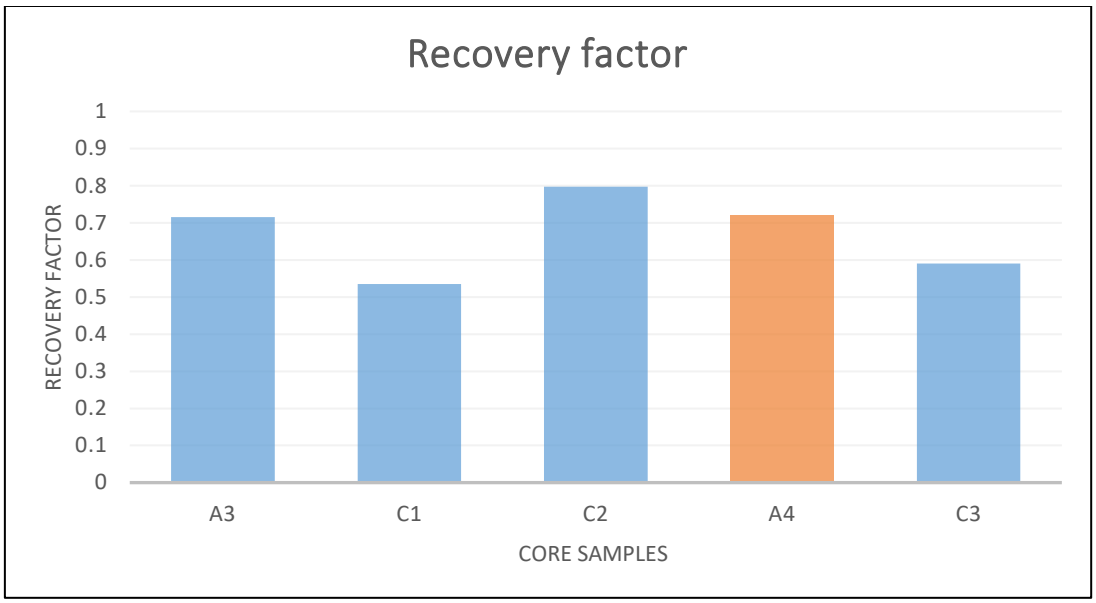


Figure 29 Recovery factors of the core samples

There is no doubt that the injection of water or brine improves the oil recovery in many ways in oil industry, but in our case here the RF looks quite high. The possible reason of this type of high RF may resulted from both a change in capillary pressure function and by a reduction of the residual oil saturation (Mass et al., 2001). In our experiments the oil is thin oil with very low viscosity and flooded by diluted brine. Some studies indicated that increase the concentration of the salt can help to lower the brine/oil IFT slightly (Valluri et al., 2016). These elements work together causes the high recovery factor at the end.

# Chapter 4 Reservoir simulation and stochastic optimization

This chapter shows the results of the numerical fluid flow simulation and optimization performed to mimic the laboratory experiments. Schlumberger software Petrel® - Eclipse® and RFD tNavigator® were used during the fluid flow simulation work for numerical modelling, and RAVEN® (Epistemy) was used for stochastic optimization.

## 4.1 Reservoir simulation

First, a static 3D model of the core plug tested in the lab was created by defining a grid with 4*10*40=1600 cells. Two wells were drilled on each side of the model: one injection and one production well. (Figure 30). This aims at mimicking the inlet and outlet of the lab core experiment.

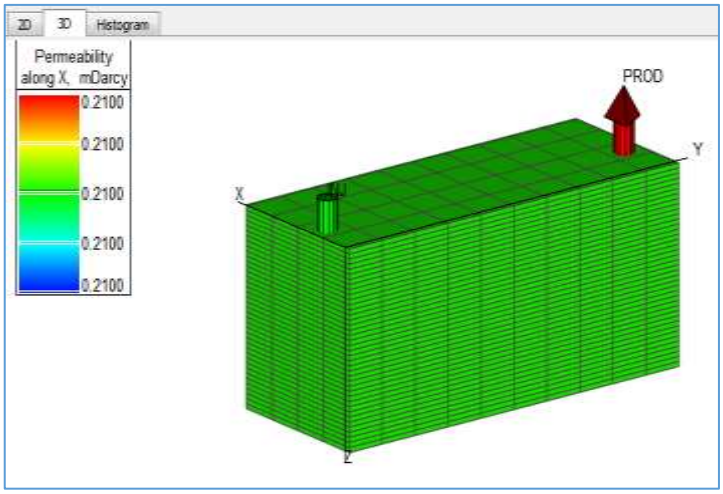


Figure 30 3D numerical model of the core plug

For upcoming reservoir simulation and history matching, petrophysical core plug parameters such as porosity and permeability were set using the lab experiments as input. Under the scope of this work, the core plug model was set to be homogeneous, which means the porosity and permeability values are the same in each cell of the model. This modelling scheme was followed due to time constrains. For a reliable modelling one

should include the natural heterogeneities of the core plug, relying for example on geostatistical simulation.

The production data which obtained from the lab was used as observed production data for history matching and comparison of the numerical simulation results.

Since the estimated rock properties from the lab experiments are similar for all the core samples, core plug C1 was used as representative of all the core samples. Original history production data of core plug C1 from the lab is imported into the simulator, shown in (a) of the Figure 31, and (b) is the cumulative oil production for plug C1.

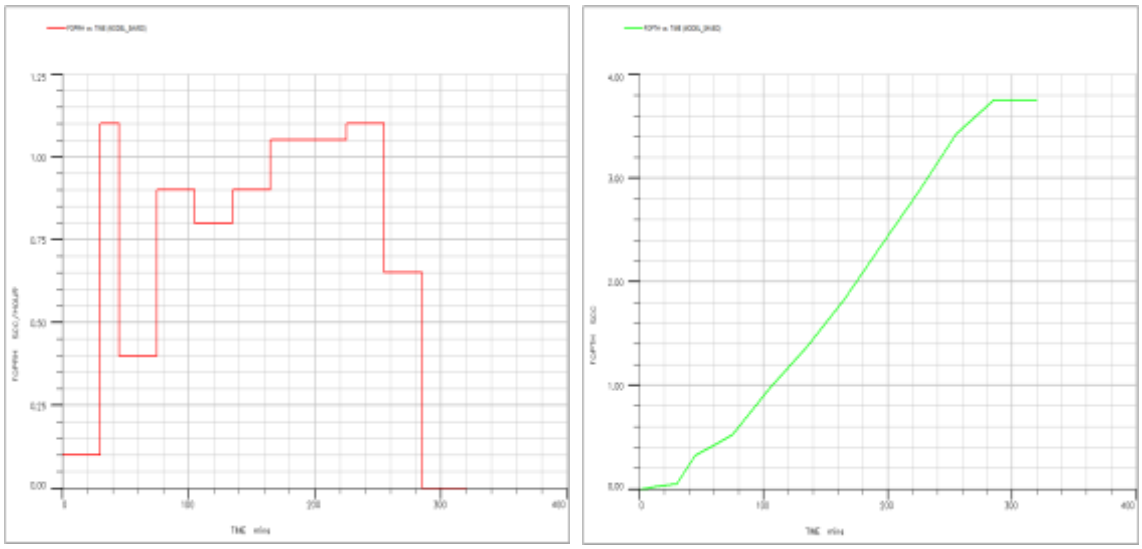

(a) History production data (b) Cumulative oil production

Figure 31 History production data

Figure 32 shows the numerical fluid flow simulation at a given time step during the water flooding.

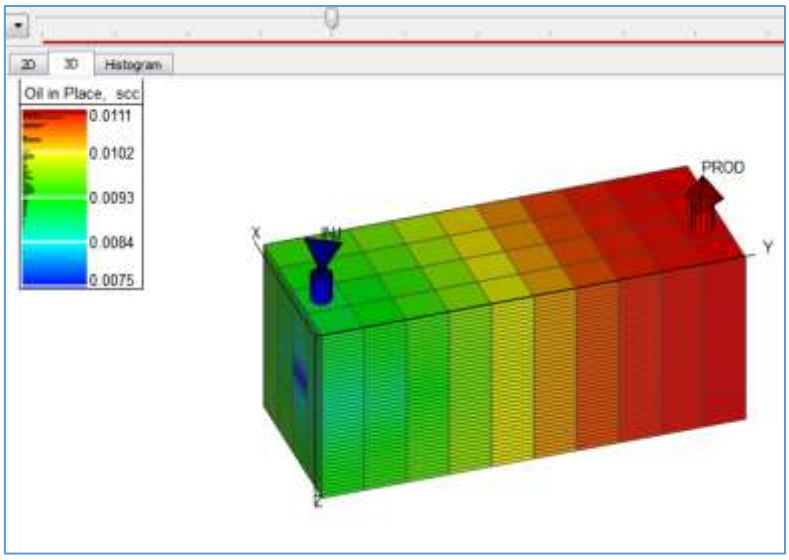


Figure 32 Water flooding process in simulator tNavigator

The simulated production profile obtained by running the fluid flow simulator is shown in Figure 33 along with the measured production data. At the beginning of the production the simulation is able to reproduce the observed data, while it fails during the latter stages of the experiment. These discrepancies can be attributed to the relatively simple approach used to model the petrophysical properties of the core sample, lack of parameterization in terms of engineering parameters of unsuitability of the fluid flow simulator in reproducing the real fluid behavior.

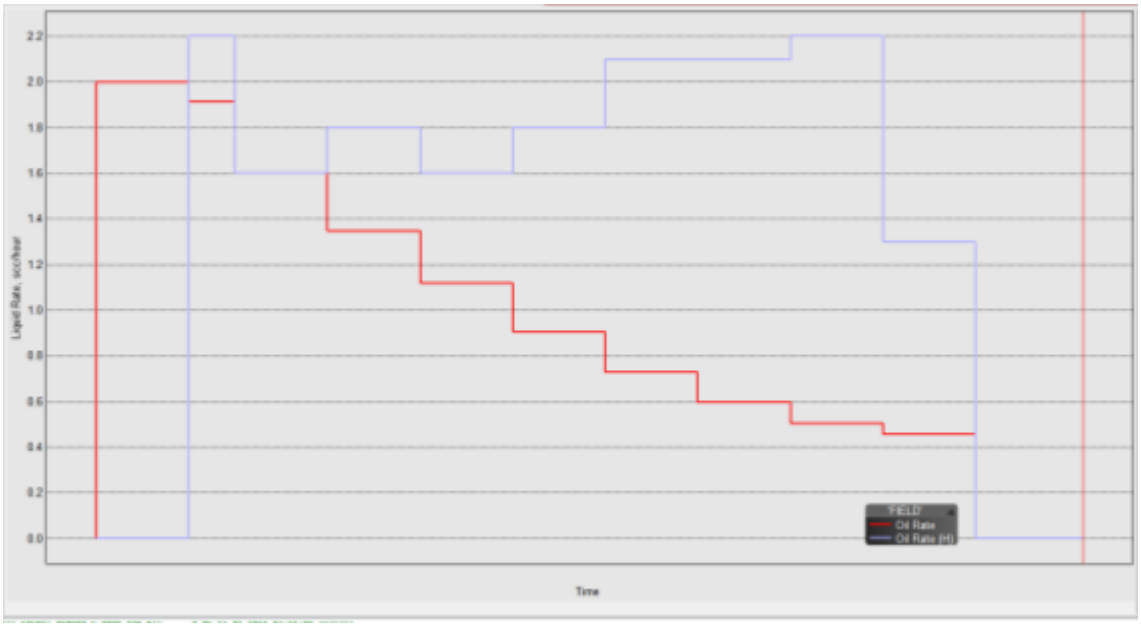


Figure 33 History production data (blue) and simulated data (red)

Improvements on the match can be done by optimizing the description of the core plug model such as porosity and permeability. In order to lift the red curve up to the blue curve, i.e. increase the simulated production, either increase the porosity or increase the permeability, or both.

### 4.2 Stochastic optimization

Particle Swarm optimization (PSO) was used to perturb and optimize the porosity and permeability values of the numerical core plug model. This simple approach considers constant petrophysical values for the entire model.

The historical production data from core sample C1 was imported during the creation of a new project for history matching. Some parameters, variables and its range should be treated very carefully, for example the standard deviation Sigma, porosity and permeability, because they have big impact on the process and result. That is why a reasonable range for porosity and permeability (Figure34) were given and some other parameters also set as below during the configuration before launch the history matching by the software RAVEN:

$\Phi_{min}$=0.01 $\Phi_{max}$=0.3 $K_{min}$=0.01mD $K_{max}$=1000 mD Sigma=0.1

$a is porosity $b, is permeabilities

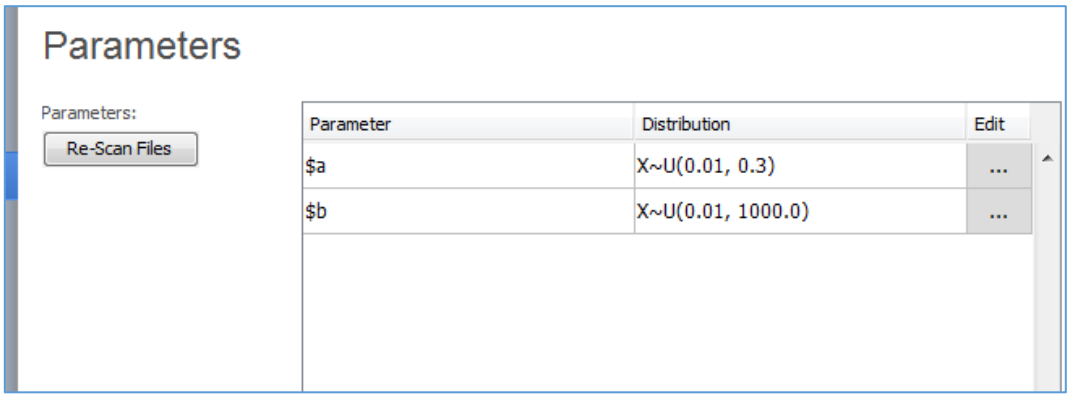


Figure 34 Parameter set up for history matching process

PSO ran with a total of 500 iterations. Figure 35 shows the convergence of the procedure. From iteration 0 to iteration 500 it is possible to interpret a decrease of the misfit function computed between observed production data from the lab and the simulated one. The five production profiles that ensured the minimum misfit value are shown in Figure 36.

From Figure 36 it is possible that the overall match between simulated and observed production curves is poor. While the general trend of the production profile at early stages is relatively well reproduced after 1,5 the product profiles diverge considerably. This behavior is somehow expected as we are modeling a complex core plug, with complex and heterogeneous distribution of porosity and permeability, with constant porosity and permeability values. The simulated production profiles indicate that most of the fluid present in the system is produced at very early stages. In addition, we are not optimizing (or defining) realistic relative permeability curves which do have a great impact on the simulation results.

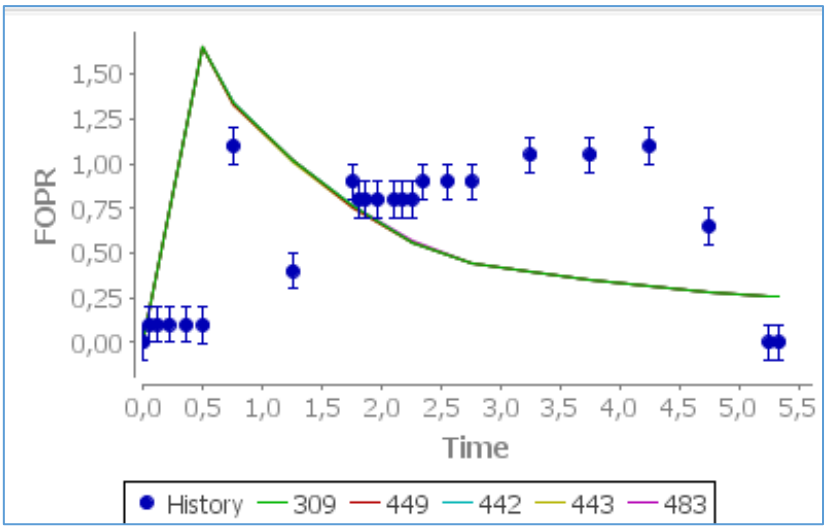


Figure 35 Comparison between observed data from lab experiments and the five best production profiles

Nevertheless, Figure 36 shows the optimized porosity and permeability values after the stochastic optimization procedure. The optimized values of porosity at the end of the iterative procedure are able to encapsulate the measured porosity value at the lab. However, the stochastic optimizer is mainly sampling values below the measured one. As

porosity was not measured with the standard mercury test the values inferred from the lab experiment are prone to uncertainties.

On the other hand, the optimized value for permeability is much larger than the one inferred from the lab. The explanation behind these differences may be related to the lack of realistic relative permeability curves or the natural heterogeneities of the core plug that were not considered (i.e. the use of a constant permeability value does not represent the true reality of connected versus unconnected pores).

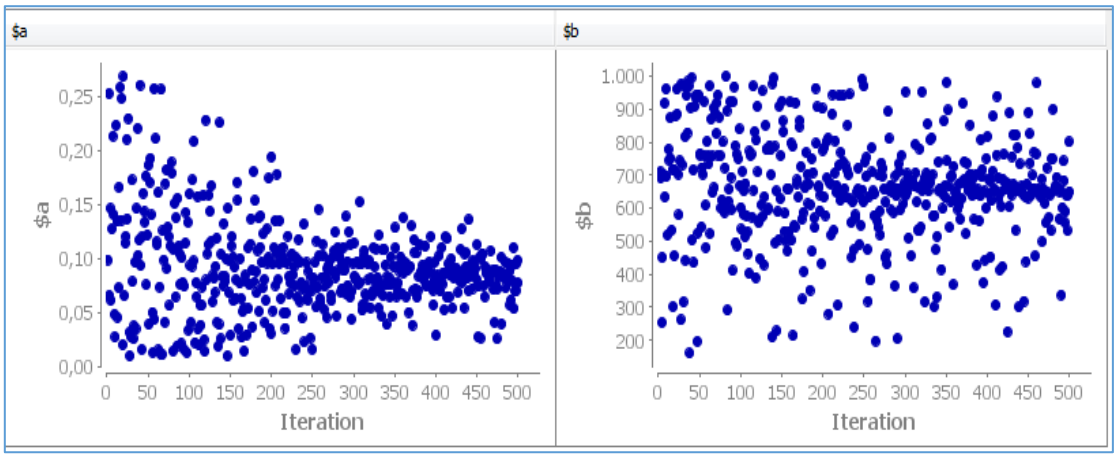


Figure 36 Evolution of porosity and permeability during the stochastic optimization

# Chapter 5 Final remarks and conclusion

For the experimental part of the research work, rock samples were collected from a limestone outcrop located in the central part of Portugal. These samples can be considered as analogue carbonate reservoir rock. The laboratory experiments included several stages which corresponds to specimen preparation, drying and saturation considering ISRM suggested methods (ISRM and Franklin, 1977). With this procedure, effective porosity was estimated for each of the seven specimens. Chapter 3.1 summarizes the experimental protocol followed to measure porosity. These values agree with those expected for these samples from previous lab studies. Table 3 and Figure 14 summarize the most important data related to porosity. One of the core sample, A4, was saturated for a long period (i.e. 23 days) and its result shows a slightly higher porosity than the remaining samples. These were saturated only for 20 hours. However, this does not have an impact on the results on the recovery factor estimated in Chapter 3.2.4. Therefore, it is still a question to be answered how much contribution comes from this longer saturation. Further study and investigation are needed to draw conclusions.

Proper working parameters of the core flooding experiment, such as confinement pressure and injection rate of the fluid were determined by preliminary tests on two samples. Absolute permeability was computed for each core after flooding with synthetic oil (Chapter 3.2.2). Results different between samples but are all within the range between 0.194 mD and 0.215mD.

Core flooding with brine experienced much higher injection pressure than flooding with synthetic oil isooctane since brine has relatively high viscosity than isooctane. Consequently, isooctane flow through the core plug much easier than brine. This phenomenon also can be inferred by the definition of viscosity (i.e. Viscosity is a term used to describe resistance to flow)

Relatively a very high oil recover was estimated for all individual specimen after core flooding. Plug C2 obtained the highest oil recovery among the five specimens after flooding experiment. Estimated pore volume of Plug C2 is about 15.2ml, cumulatively

produced oil is about 12.1ml, and this made the recovery factor reaches almost 80%. Lowest recovery factor among these samples is 0.53(Figure29)

Errors and uncertainties may occur during the whole process of the lab experiment. These uncertainties are present since the core preparation until the end of the core flooding test. For example, the way of the measurement, accuracy of the equipment and tools, scales and reading. Also, some errors may come from the special property of the fluid such as evaporation of the isooctane. The following mitigation procedures were introduced for minimizing the error and uncertainties during the lab test:

a) Weight and size of each core were measured five times for each and took the average for the calculation.
b) Standard procedure or suggested method were applied for the lab experiments, for example ISRM suggested method was introduce for specimen preparation and porosity calculation.
c) Use of proper cover for the fluid receiver to avoid the isooctane evaporation.

Some improvements can be done in the future for better and more accurate results, for example using digital pressure gauge on inlet and outlet of the core holder because small error may result from reading and estimating. Also, real-time data acquisition should be considered to minimize measuring errors. Temperature condition establishes for the test which can mimic the reservoir temperature.

The second stage of this thesis comprised the reproduction of the lab experiments in a numerical fluid flow simulator. The production data obtained from the lab experiments was considered as real historical production data in a stochastic history matching optimization using a simplified 3D core plug model with constant porosity and permeability (Chapter4.1).

The stochastic history matching used Particle Swarm Optimization to sample from a prior uniform distribution of porosity and permeability. The match obtained is considerably good at the beginning of the production of the history. However, the matching accuracy decreases as the production time increases. This might be caused by the simplistic approach when modelling the petrophysical properties of the core samples.

As future work, I propose the use of geostatistical modelling to get a reliable spatial distribution of porosity and permeability within the core sample numerical model. This is expected to increase the match of the observed production data.

## References

Ahmed, T., 2001; Reservoir engineering handbook, Gulf Professional Publishing.

Almeida, A. E. M. V. F., 2018; Correlação entre a extensão volumétrica e a porosidade em rochas calcárias saturadas, Master thesis, Instituto Superior Técnico, University of Lisbon.

Amyx J.W., Bass Jr. D.M., Whiting R.L., 1960; Petroleum Reservoir Engineering, McGraw-Hill.

Avasare, M., 2016; Digital Rock Physics for Core flooding Simulations, Master thesis, Instituto Superior Técnico, University of Lisbon.

Carvalho, M., Serra, L., M., Lozano, M., A., 2011; Optimal synthesis of trigeneration systems subject to environmental constraints, Elsevier.

Cossé, R., 1993; Basics of Reservoir Engineering- Oil and Gas Field Development Techniques, Butterworth-Heinemann.

Ertekin, T., Abou-Kassem J.H., King G.R., 2001; Basic Applied Reservoir Simulation, Society of Petroleum Engineers.

Gilman, J., Ozgen, C., 2013; Reservoir Simulation: History Matching and Forecasting, Society of Petroleum Engineers.

Guo, B., Liu X., Tan, X., 2017; Petroleum Production Engineering, Gulf Professional Publishing.

Graue, A., 2006; Experimental Reservoir Physics, Lab Manual, Ptek 214, Department of Physics and Technology, University of Bergen

ISRM, Franklin, J.A., 1977; Suggested methods for determining water content, porosity, density, absorption and related properties and swelling and slake-durability index properties, Pergamon.

Majod, A. A., Saidian, M., Prasad, M., Koh, C. A., 2015; Measurement of the Water Droplet Size in Water-in-Oil Emulsions Using Low Field Nuclear Magnetic Resonance for Gas Hydrate Slurry Application, Canadian Journal of Chemistry.

Kennedy, J., Eberhart, R., 1995; Particle swarm optimization, International Conference on Neural Networks

Lyons, W., 1996; Standard Handbook of Petroleum and Natural Gas Engineering: Volume 2, Gulf Professional Publishing.

Manuppella, G., Barbosa, B., Azerêdo, A. C., Carvalho, J., Crispim, J., Machado, S., Sampaio, J., 2006; Notícia Explicativa da Folha 27-C Torres Novas, Instituto Nacional de Engenharia, Tecnologia e Inovação, Departamento de Geologia. Lisboa.

Santos, T. R., 2017; Estudo laboratorial das propriedades poroelásticas da rocha do calcário do Codaçal, Master thesis, Instituto Superior Técnico, University of Lisbon.

Maas, J. G., Wit, K., Morrow, N. R., 2001; Enhanced oil recovery by dilution of injection brine: Future interpretation of experimental results, SCA.

McPhee, C., Reed, J., Zubizarreta, I., 2015; Core Analysis - A Best Practice Guide, Volume 64, Elsevier

Mohamed, L., Christie, M., Demyanov, V., 2010; Comparison of Stochastic Sampling Algorithms for Uncertainty Quantification, Society of Petroleum Engineers.

Kestin, J. H., Khalifa, H. E., Correia, R. j., 1981; Tables of the dynamic and kinematic viscosity of aqueous NaCl solutions in the temperature range 20–150 °C and the pressure range 0.1–35 MPa , Journal of Physical and Chemical Reference Data.

Rabiei, A., Sharifinik, M., Niazi, A., Hashemi, A., Ayatollahi, S., 2013; Core flooding tests to investigate the effects of IFT reduction and wettability alteration on oil recovery during MEOR process in an Iranian oil reservoir, Springer.

Rodrigues, M. L., 1998; Evolução geomorfológica quaternária e dinâmica actual-Aplicações ao ordenamento do território. Exemplos no Maciço Calcário Estremenho, Dissertação de Doutoramento em Geografia Física, Faculdade de Letras da Universidade de Lisboa. Lisboa. 868 pp.

Silverstein, T. P., 1998; The Real Reason Why Oil and Water Don’t Mix, Journal of Chemical Educatio.

Tavakoli, V., 2018; Geological Core Analysis: Application to Reservoir Characterization, Springer-Briefs in Petroleum Geoscience & Engineering.

Valluri, M. K., Alvarez, J. O., Schechter D. S.,2016; Study of the Rock/Fluid Interactions of Sodium and Calcium Brines with Ultra-Tight Rock Surfaces and their Impact on Improving Oil Recovery by Spontaneous Imbibition, Society of Petroleum Engineers.

# Appendix A

Table A- 1 Weight measurements data during the drying

| Hours in the Oven | Measured weight(g) of the plug | | | |
|---|---|---|---|---|
| | Plug A1 | PlugA2 | PlugA3 | PlugA4 |
| 0 | 263,99 | 261,68 | 263,41 | 262,38 |
| 17 | 254,37 | 251,04 | 254,66 | 252,98 |
| 21 | 254,37 | 251,04 | 254,65 | 252,98 |
| 24 | 254,36 | 251,03 | 254,64 | 252,98 |

Table A- 2 Estimated porosity of core samples (Effective)

| Estimated porosity of core samples (Effective) | | | | | | | |
|---|---|---|---|---|---|---|---|
| Core plug | A1 | A2 | A3 | A4 | C1 | C2 | C3 |
| Porosity | 0,138 | 0,145 | 0,136 | 0,148 | 0,136 | 0,139 | 0,143 |

Table A- 3 some important values on porosity estimation

| | |
|---|---|
| Minimum Ø | 0,136 |
| Max Ø | 0,1484 |
| Mean value of Ø | 0,1407 |
| Standard deviation | 0,00443 |

Table A- 4 Comparison of the recovery factors

| Core sample | Pore volume (ml) | Total produced oil (ml) | Recovery factors |
|---|---|---|---|
| A3 | 15,1 | 10,8 | 0,715 |
| C1 | 14,8 | 7,95 | 0,535 |
| C2 | 15,2 | 12,1 | 0,797 |
| A4 | 16,5 | 11,9 | 0,722 |
| C3 | 15,5 | 9,15 | 0,590 |

# Appendix B

Table B- 1 Estimated absolute permeability to isooctane for Plug A3

| Absolute permeability estimation via Isooctane flooding on Plug A3 | | | | |
|---|---|---|---|---|
| Duration (minute) | Confine pressure (bar) | Flow rate (ml/h) | Inlet Pressure (bar) | Respective permeability (mD) |
| 60 | 100 | 15 | 10.3 | 0.214 |
| 60 | 100 | 20 | 13.3 | 0.215 |
| 60 | 100 | 25 | 16.3 | 0.216 |

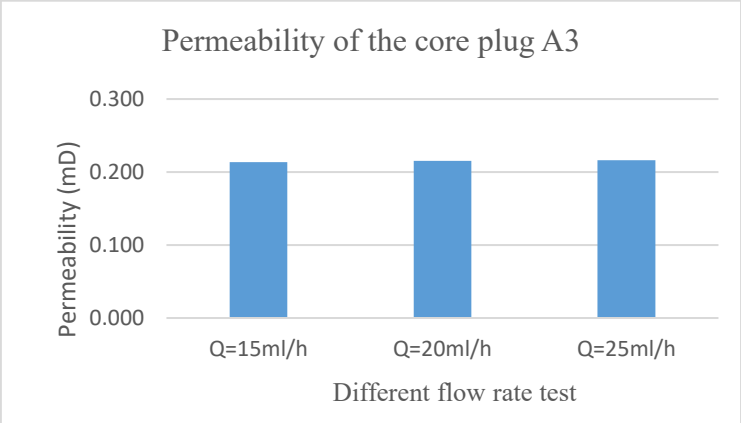


Figure B- 1 Estimated absolute permeability to isooctane for plug A3

Table B- 2 Estimated absolute permeability to isooctane for Plug A4

| Absolute permeability estimation via Isooctane flooding on Plug A4 | | | | |
|---|---|---|---|---|
| Duration (minute) | Confine pressure (bar) | Flow rate (ml/h) | Inlet Pressure (bar) | Respective permeability(mD) |
| 40 | 100 | Q=15ml/h | 10.3 | 0,215 |
| 30 | 100 | Q=20ml/h | 13.5 | 0,213 |
| 40 | 100 | Q=25ml/h | 17 | 0,208 |

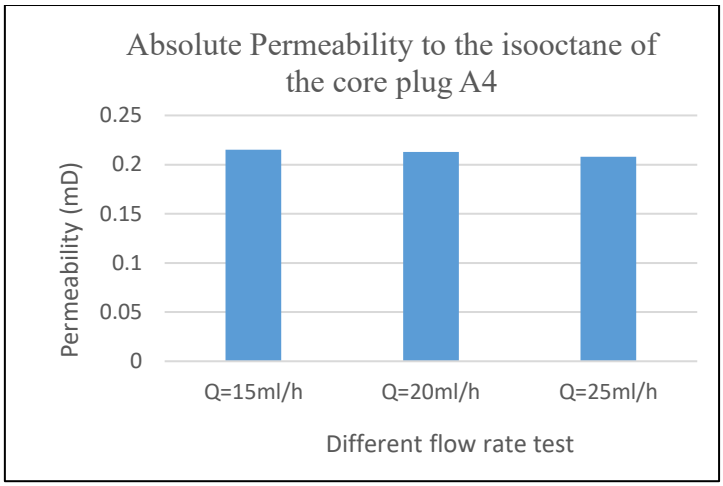


Figure B- 2 Estimated absolute permeability to isooctane for Plug A4

Table B- 3 Estimated absolute permeability to isooctane for Plug C1

| Estimated absolute permeability to isooctane for Plug C1 | | | | |
|---|---|---|---|---|
| Duration (minute) | Confine pressure (bar) | Flow rate (ml/h) | Inlet Pressure (bar) | Respective permeability(mD) |
| 40 | 100 | Q=15ml/h | 10.3 | 0,215 |
| 30 | 100 | Q=20ml/h | 13.5 | 0,213 |
| 40 | 100 | Q=25ml/h | 17 | 0,208 |

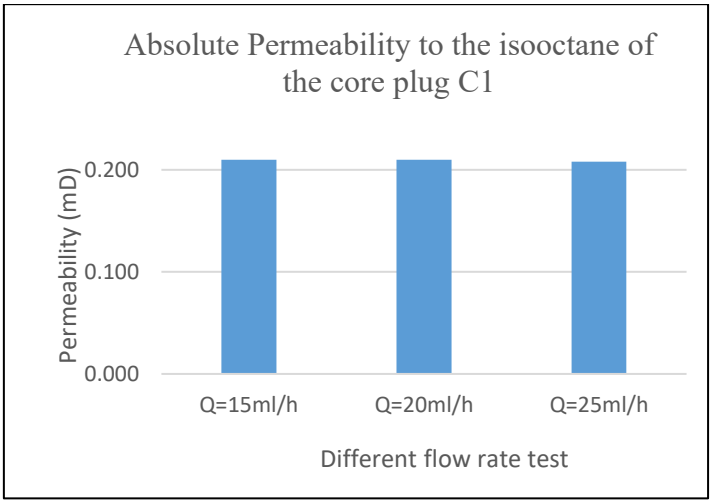


Figure B- 3 Estimated absolute permeability to isooctane for Plug C1

Table B- 4 Estimated absolute permeability to isooctane for Plug C2

| Estimated absolute permeability to isooctane for Plug C2 | | | | |
|---|---|---|---|---|
| Duration (minute) | Confine pressure (bar) | Flow rate (ml/h) | Inlet Pressure (bar) | Respective permeability(mD) |
| 35 | 100 | Q=15ml/h | 15 | 0.182 |
| 45 | 100 | Q=20ml/h | 20 | 0,186 |
| 85 | 100 | Q=25ml/h | 25 | 0,213 |

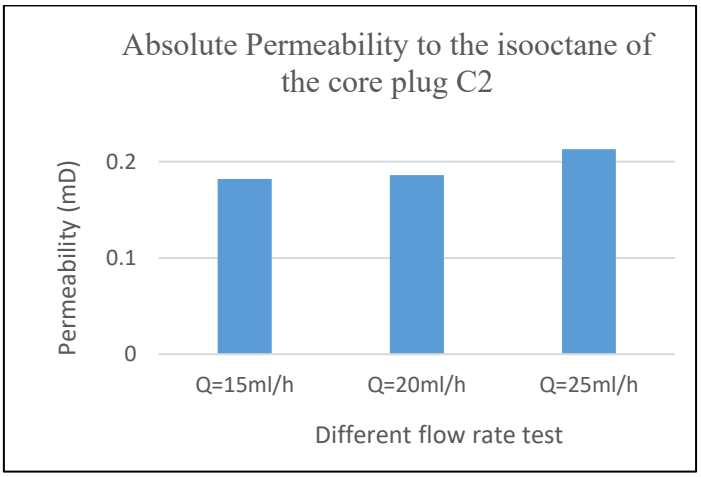


Figure B- 4 Estimated absolute permeability to isooctane for Plug C2

Table B- 5 Estimated absolute permeability to isooctane for Plug C3

| Absolute permeability estimation via Isooctane flooding on Plug C3 | | | | |
|---|---|---|---|---|
| Duration (minute) | Confine pressure (bar) | Flow rate (ml/h) | Inlet Pressure (bar) | Respective permeability(mD) |
| 40 | 100 | Q=15ml/h | 11 | 0.200 |
| 30 | 100 | Q=20ml/h | 13.9 | 0,206 |
| 30 | 100 | Q=25ml/h | 18 | 0,196 |

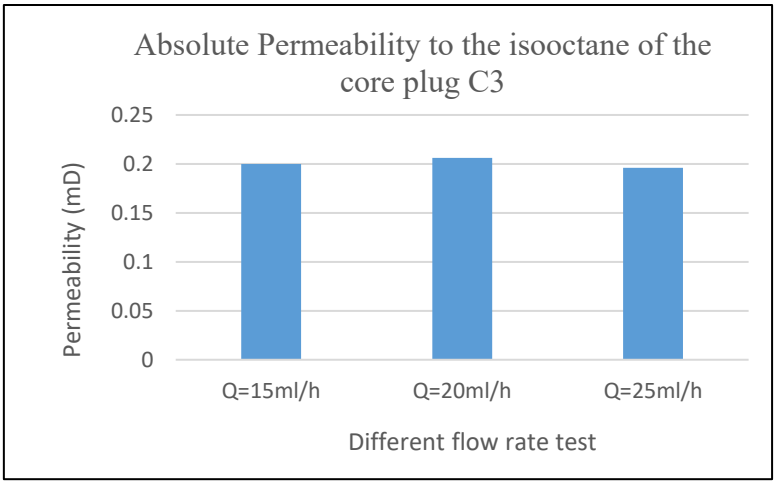


Figure B- 5 Estimated absolute permeability to isooctane for Plug C3

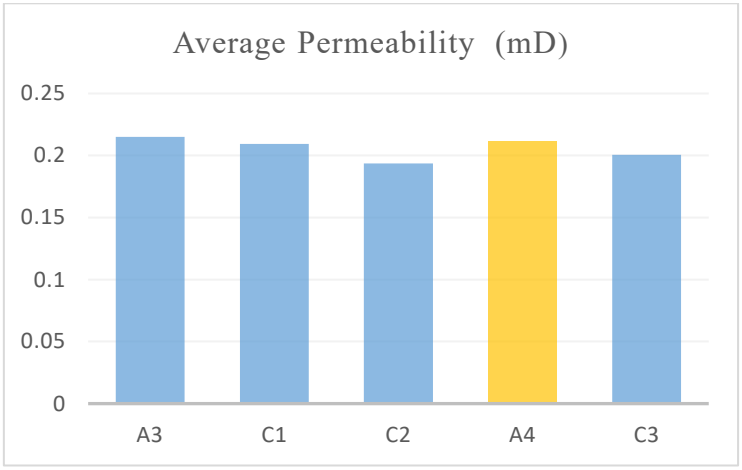


Figure B- 6 Average absolute permeability to isooctane for all five plugs

## Appendix C

Table C- 1 Production data of core flooding with brine of core plug A3

| Core flooding with brine for Plug A3 | | | | | | |
|---|---|---|---|---|---|---|
| Time (minute) | Injection rate (ml/h) | Injection Pressure (bar) | Produced isooctane (ml) | Production rate (Isooctane)(ml/h) | Production rate (brine)(ml/h) | Produced brine (ml) |
| 0 | 0 | 0 | 0 | 0 | 0 | 0 |
| 10 | 2 | 1,8 | 0,4 | 2,4 | 0 | 0 |
| 40 | 2 | 4 | 0,8 | 1,60 | 0 | 0 |
| 50 | 2 | 5,7 | 0,2 | 1,20 | 0 | 0 |
| 60 | 2 | 6,8 | 0,4 | 2,40 | 0 | 0 |
| 70 | 2 | 7,8 | 0,2 | 1,20 | 0 | 0 |
| 80 | 2 | 8,8 | 0,3 | 1,80 | 0 | 0 |
| 95 | 2 | 10 | 0,5 | 2,00 | 0 | 0 |
| 105 | 2 | 11,8 | 0,3 | 1,80 | 0 | 0 |
| 115 | 2 | 12,5 | 0,3 | 1,80 | 0 | 0 |
| 125 | 2 | 14 | 0,3 | 1,80 | 0 | 0 |
| 135 | 2 | 15 | 0,3 | 1,80 | 0 | 0 |
| 151 | 2 | 17 | 0,5 | 1,88 | 0 | 0 |
| 161 | 2 | 18 | 0,3 | 1,80 | 0 | 0 |
| 173 | 2 | 19,3 | 0,4 | 2,00 | 0 | 0 |
| 180 | 2 | 20 | 0,2 | 1,71 | 0 | 0 |
| 192 | 2 | 21 | 0,3 | 1,50 | 0 | 0 |
| 202 | 2 | 22 | 0,4 | 2,40 | 0 | 0 |
| 212 | 2 | 22,5 | 0,2 | 1,20 | 0 | 0 |
| 222 | 2 | 20 | 0,3 | 1,80 | 0 | 0 |
| 232 | 2 | 21 | 0,3 | 1,80 | 0 | 0 |
| 242 | 2 | 21,8 | 0,2 | 1,20 | 0 | 0 |
| 252 | 2 | 22 | 0,3 | 1,80 | 0 | 0 |
| 262 | 2 | 23 | 0,3 | 1,80 | 0 | 0 |
| 272 | 2 | 23,7 | 0,3 | 1,80 | 0 | 0 |
| 282 | 2 | 23,8 | 0,2 | 1,20 | 0 | 0 |
| 292 | 2 | 24 | 0,4 | 2,40 | 0 | 0 |
| 302 | 2 | 24 | 0,3 | 1,80 | 0 | 0 |
| 332 | 2 | 24 | 0,3 | 0,60 | 0 | 0 |
| 342 | 2 | 24 | 0,3 | 1,80 | 0 | 0 |
| 352 | 2 | 24 | 0,4 | 2,40 | 0 | 0 |
| 362 | 2 | 24 | 0,3 | 1,80 | 0 | 0 |
| 410 | 2 | 24 | 0,3 | 0,38 | 0 | 0 |
| 422 | 2 | 24 | 0,3 | 1,50 | 0 | 0 |
| 432 | 2 | 24,5 | 0 | 0,00 | 0 | 0 |
| 442 | 2 | 24,5 | 0 | 0,00 | 2,40 | 0,4 |
| 452 | 2 | 24,5 | 0 | 0,00 | 1,80 | 0,3 |
| 462 | 2 | 24,5 | 0 | 0,00 | 1,80 | 0,3 |
| 472 | 2 | 24,5 | 0 | 0,00 | 1,20 | 0,2 |

Table C- 2 Production data of core flooding with brine of core plug C1

| Core flooding with brine for Plug C1 (Saturated with synthetic oil for 20 hours) | | | | | | |
|---|---|---|---|---|---|---|
| Time (minute) | Injection rate (ml/h) | Injection Pressure (bar) | Produced oil (ml) | Production rate (oil) (ml/h) | Production rate (brine) (ml/h) | Produced brine(ml) |
| 0 | 0 | 0 | 0 | 0 | 0 | 0 |
| 30 | 2 | 12 | 1,1 | 2,2 | 0 | 0 |
| 45 | 2 | 12,7 | 0,4 | 1,6 | 0 | 0 |
| 75 | 2 | 15 | 0,9 | 1,8 | 0 | 0 |
| 105 | 2 | 18 | 0,8 | 1,6 | 0 | 0 |
| 135 | 2 | 22 | 0,9 | 1,8 | 0 | 0 |
| 165 | 2 | 25 | 1,05 | 2,1 | 0 | 0 |
| 195 | 2 | 25 | 1,05 | 2,1 | 0 | 0 |
| 225 | 2 | 25 | 1,1 | 2,2 | 0 | 0 |
| 255 | 2 | 25 | 0,65 | 1,3 | 0 | 0 |
| 285 | 2 | 25 | 0 | 0 | 0,3 | 0,15 |
| 315 | 2 | 25 | 0 | 0 | 2,4 | 1,2 |

Table C- 3 Production data of core flooding with brine of core plug C2

| Core flooding with brine for Plug C2 (Saturated with synthetic oil for 20 hours) | | | | | | |
|---|---|---|---|---|---|---|
| Time (minute) | Injection rate (ml/h) | Injection Pressure (bar) | Produced isooctane (ml) | Production rate (oil) (ml/h) | Production rate(brine) (ml/m) | Produced brine(ml) |
| 0 | 0 | 0 | 0 | 0 | 0 | 0 |
| 60 | 2 | 1,3 | 0,8 | 0,8 | 0 | 0 |
| 120 | 2 | 5,8 | 1,8 | 1,80 | 0 | 0 |
| 180 | 2 | 10 | 1,8 | 1,80 | 0 | 0 |
| 225 | 2 | 12,3 | 1,4 | 1,87 | 0 | 0 |
| 255 | 2 | 14 | 0,7 | 1,40 | 0 | 0 |
| 285 | 2 | 16,5 | 0,9 | 1,80 | 0 | 0 |
| 315 | 2 | 19 | 1 | 2,00 | 0 | 0 |
| 345 | 2 | 20 | 1 | 2,00 | 0 | 0 |
| 375 | 2 | 20 | 1 | 2,00 | 0 | 0 |
| 387 | 2 | 20 | 0,6 | 3,00 | 0 | 0 |
| 405 | 2 | 20 | 0,7 | 2,33 | 0 | 0 |
| 418 | 2 | 20 | 0,4 | 1,85 | 0 | 0 |
| 482 | 2 | 20 | 0 | 0,00 | 2,00 | 0,1 |
| 512 | 2 | 20 | 0 | 0,00 | 2,00 | 1 |

Table C- 4 Production data of core flooding with brine of core plug C3

| Core flooding with brine for Plug C3 (Saturated with synthetic oil for 20 hours) | | | | | | |
|---|---|---|---|---|---|---|
| Time (minute) | Injection rate (ml/h) | Injection Pressure (bar) | Produced oil (ml) | Production rate (oil)(ml/h) | Production rate(brine) (ml/h) | Produced brine (ml) |
| 0 | 0 | 0 | 0 | 0 | 0 | 0 |
| 30 | 2 | 12 | 0,9 | 1,8 | 0 | 0 |
| 60 | 2 | 14,8 | 1 | 2,00 | 0 | 0 |
| 90 | 2 | 17,5 | 0,9 | 1,80 | 0 | 0 |
| 120 | 2 | 20 | 1 | 2,00 | 0 | 0 |
| 150 | 2 | 21,5 | 0,8 | 1,60 | 0 | 0 |
| 180 | 2 | 27 | 0,8 | 1,60 | 0 | 0 |
| 210 | 2 | 27 | 0,8 | 1,60 | 0 | 0 |
| 240 | 2 | 27 | 1 | 2,00 | 0 | 0 |
| 270 | 2 | 27 | 0,95 | 1,90 | 0 | 0 |
| 300 | 2 | 27 | 0,7 | 1,80 | 0,40 | 0,2 |
| 314 | 2 | 27 | 0,3 | 1,71 | 0,43 | 0,1 |
| 372 | 2 | 27 | 0 | 0,00 | 1,03 | 1 |
| 402 | 2 | 27 | 0 | 0,00 | 2,00 | 1 |

Table C- 5 Production data of core flooding with brine of core plug A4

| Core flooding with brine for Plug A4 (Saturated with synthetic oil for 23 days) | | | | | | |
|---|---|---|---|---|---|---|
| Time (minute) | Injection rate (ml/h) | Injection Pressure (bar) | Produced oil (ml) | Production rate (oil) (ml/h) | Production rate (brine) (ml/h) | Produced brine (ml/h) |
| 0 | 0 | 0 | 0 | 0 | 0 | 0 |
| 30 | 2 | 3 | 1,4 | 2,8 | 0 | 0 |
| 60 | 2 | 6 | 0,9 | 1,80 | 0,00 | 0 |
| 90 | 2 | 8,6 | 0,9 | 1,80 | 0,00 | 0 |
| 120 | 2 | 11 | 0,9 | 1,80 | 0,00 | 0 |
| 150 | 2 | 13,7 | 1 | 2,00 | 0,00 | 0 |
| 180 | 2 | 15,8 | 0,9 | 1,80 | 0,00 | 0 |
| 210 | 2 | 17,9 | 0,9 | 1,80 | 0,00 | 0 |
| 240 | 2 | 19,8 | 0,8 | 1,60 | 0,00 | 0 |
| 270 | 2 | 25 | 0,9 | 1,80 | 0,00 | 0 |
| 300 | 2 | 26,2 | 1 | 2,00 | 0,00 | 0 |
| 330 | 2 | 26,2 | 1 | 2,00 | 0,00 | 0 |
| 360 | 2 | 26,2 | 1 | 2,00 | 0,00 | 0 |
| 375 | 2 | 26,2 | 0,3 | 1,20 | 0,00 | 0 |
| 461 | 2 | 26,2 | 0 | 0,00 | 1,76 | 1 |